LAWRENCE
LIVERMORE
NATIONAL
LABORATORY

UCRL-TR-229495

Evaluation of ITER MSE Viewing Optics

S. Allen, S. Lerner, K. Morris, J. Jayakumar, C. Holcomb, M. Makowski, J. Latkowski, R. Chipman

March 28, 2007

This work was performed under the auspices of the U.S. Department of Energy by University of California, Lawrence Livermore National Laboratory under Contract W-7405-Eng-48.

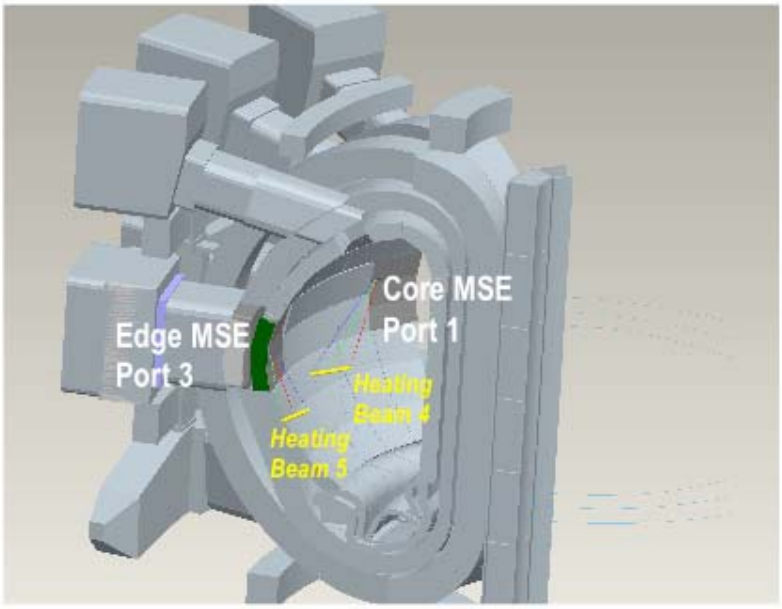

Evaluation of ITER MSE Viewing Optics

A LLNL Work for Others Project

Subcontract to PPPL ICP006860-A

PPPL 73501DD1533A

WBS Element 1.5.3.3

Project Team

S. Allen - Physics and Project overview
- S. Lerner - Optical Design
- K. Morris - Mechanical Interface, neutronics grid
- J. Jayakumar - Beam into Gas Calibration
- C. Holcomb - Measurement of Dielectric Mirror
- M. Makowski - Neutronics Design (not funded)
- J. Latkowski - Neutronics assessment (not funded)
- R. Chipman (Univ. Arizona) - Calibration (not funded)

Executive Summary

The Motional Stark Effect (MSE) diagnostic on ITER determines the local plasma current density by measuring the polarization angle of light resulting from the interaction of a high energy neutral heating beam and the tokamak plasma. This light signal has to be transmitted from the edge and core of the plasma to a polarization analyzer located in the port plug. The optical system should either preserve the polarization information, or it should be possible to reliably calibrate any changes induced by the optics.

This LLNL Work for Others project for the US ITER Project Office (USIPO) is focused on the design of the viewing optics for both the edge and core MSE systems. Several design constraints were considered, including: image quality, lack of polarization aberrations, ease of construction and cost of mirrors, neutron shielding, and geometric layout in the equatorial port plugs. The edge MSE optics are located in ITER equatorial port 3 and view Heating Beam 5, and the core system is located in equatorial port 1 viewing heating beam 4. The current work is an extension of previous preliminary design work completed by the ITER central team (ITER resources were not available to complete a detailed optimization of this system, and then the MSE was assigned to the US).

The optimization of the optical systems at this level was done with the ZEMAX optical ray tracing code. The final LLNL designs decreased the “blur” in the optical system by nearly an order of magnitude, and the polarization blur was reduced by a factor of 3. The mirror sizes were reduced with an estimated cost savings of a factor of 3. The throughput of the system was greater than or equal to the previous ITER design. It was found that optical ray tracing was necessary to accurately measure the throughput. Metal mirrors, while they can introduce polarization aberrations, were used close to the plasma because of the anticipated high heat, particle, and neutron loads. These mirrors formed an intermediate image that then was relayed out of the port plug with more ideal (dielectric) mirrors. Engineering models of the optics, port plug, and neutral beam geometry were also created, using the CATIA ITER models. Two video conference calls with the USIPO provided valuable design guidelines, such as the minimum distance of the first optic from the plasma.

A second focus of the project was the calibration of the system. Several different techniques are proposed, both before and during plasma operation. Fixed and rotatable polarizers would be used to characterize the system in the no-plasma case. Obtaining the full modulation spectrum from the polarization analyzer allows measurement of polarization effects and also MHD plasma phenomena. Light from neutral beam interaction with deuterium gas (no plasma) has been found useful to determine the wavelength of each spatial channel.

The status of the optical design for the edge (upper) and core (lower) systems are included in the following figure. Several issues should be addressed by a follow-on study, including whether the optical labyrinth has sufficient neutron shielding and a detailed polarization characterization of actual mirrors.

Table of Contents

1. Introduction

This report is a summary of the work performed on an optical design for the ITER Motional Stark Effect (MSE) viewing optics. The MSE is a US diagnostic used to measure the plasma current profile. The ITER team has established the basic measurements requirements for the MSE, and these are shown in Table I. The basic MSE

MEASUREMENT	PARAMETER	CONDITION	RANGE or COVERAGE	RESOLUTION		ACCURACY
25. Current Profile	q(r)	Physics study	0.5 - 5	10 ms	a/20	10 %
			5 – TBD	10 ms	a/20	0.5
	r(q=1.5,2) / a	NTM feedback	0.3 – 0.9	10 ms	–	5 cm / a
	$r(q_{min})/a$	Reverse shear control	0.3 – 0.7	1 s	–	5 cm / a

Table 1 MSE measurement requirements from ITER documentation

measurement technique is shown in Fig. 1. A deuterium neutral beam interacts with the plasma and a visible spectrum is created. This D_α visible light, which is shifted in wave-

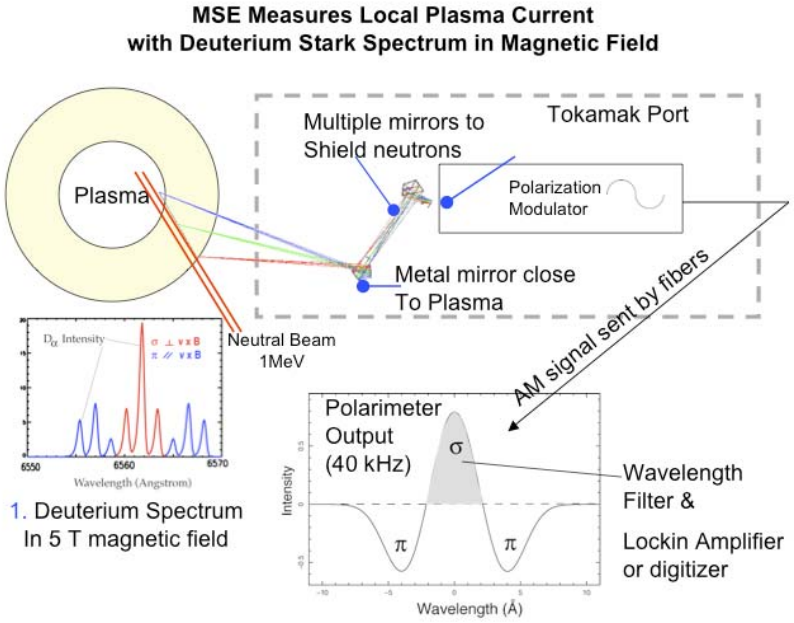

Figure 1-1. Schematic of a typical MSE measurement

length due to the Doppler effect, has both σ (parallel to $v \times B$) and π (perpendicular to $v \times B$) components, which are further split in wavelength. The polarization angle of the polarized light is related to the local magnetic field, and thereby the local plasma current density. As shown in Figure 1-1., the polarized light is collected by optics and relayed to a polarization modulator-analyzer. These optics must preserve the polarization information, and also be located so that the neutron shielding of the port plug is maintained. It is envisioned that an optical labyrinth, using metal mirrors close to the plasma and dielectric mirrors farther away in the port plug, will accomplish both of these tasks. The neutron-shielding requirement drives the design to multiple mirrors with nearly right angles, and the polarization preservation requirement drives the design to fewer mirrors. The Stark multiplet is next analyzed for polarization with a pair of Photo-Elastic Modulators (PEM); these essentially convert the polarization information into an amplitude-modulated signal. As shown in Fig. 1-1, the σ component becomes a positive signal, and the π components are negative signals. With purely linear polarization, the modulation of the crystal in the PEM at a frequency f (typically 20 kHz) results in a signal at 2f (40 Khz). This AM signal can be analyzed with a lock-in amplifier or the whole frequency spectrum can be acquired and post-processed. The later technique has the advantage that MHD modes in the plasma can be analyzed (appearing at $2f+f_{MHD}$), and additional information about the polarization properties of the optical train can be obtained (e.g., circular polarization appears at a frequency of f).

The ITER team also established a baseline design which was summarized in several publications, most notably summarized in [1]. The concept at this stage was to

have two MSE systems, a core and an edge system, viewing two different neutral beams. Shown in Fig. 1-2 (reprinted from [1]) is a plan view of the ITER MSE system.

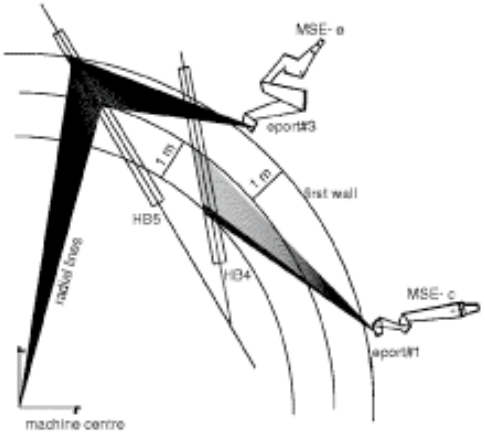

FIG. 1. Plan view of the MSE edge and core arrangement. Two periscopes look at different HNBs providing best spatial resolution and complementing plasma coverage. Eport3 periscope is placed above the HNB 4 level.

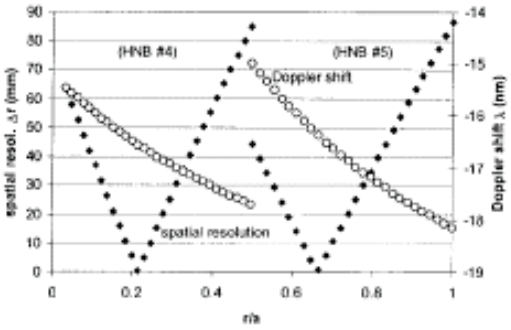

FIG. 2. Spatial resolution (black squares) and Doppler shift (open circles) for the MSE-e (HNB 5) and MSE-c (HNM 4).

Figure 1-2. Original ITER Design (designated as “EU”).

On the left in Figure 1-2 is a schematic of the core MSE system, which views heating beam 4 (HB4) from Equatorial Port 1 (eport1), and the edge system, which views heating beam 5 (HB5) from Equatorial Port 3 (eport3). A lot of careful thought and planning went into this design, as detailed in [1]. The spatial resolution and Doppler shift as a function of minor radius (r/a) are shown at the right in Figure 1-2. The spatial resolution various from a minimum of a few mm at r/a = 0.2 (core) and r/a=0.65(edge), to over 50mm at a distance of r/a~ ±.0.1 away from this minimum. The Doppler shift varies from -15 to -18 nm relative to the D_a rest wavelength.

The design activity of this SOW focuses on the optical train from the plasma to the input of the polarization analyzer, as shown in Fig. 1-1. We started with the edge system, as we had obtained the ZEMAX optical ray tracing code output from the ITER US Project Office (USIPO). It was understood that this was a “starting”, reference design,

and extensive, multi-parameter optimizations had not been done by the ITER team. For simplicity, we called this the “EU design” and we examined the optical performance with the same tools as the ITER team – the ZEMAX optical ray tracing code.

Section 2 *Using optical design parameters available from the Team Leader, create an optical model including polarization analysis*

This section deals with the establishment of the previous ITER MSE optical design for the edge system to be used as a reference for design tradeoff studies that will be presented in the following section. We obtained ZEMAX files from the US Team Leader for the optical design of the edge system.

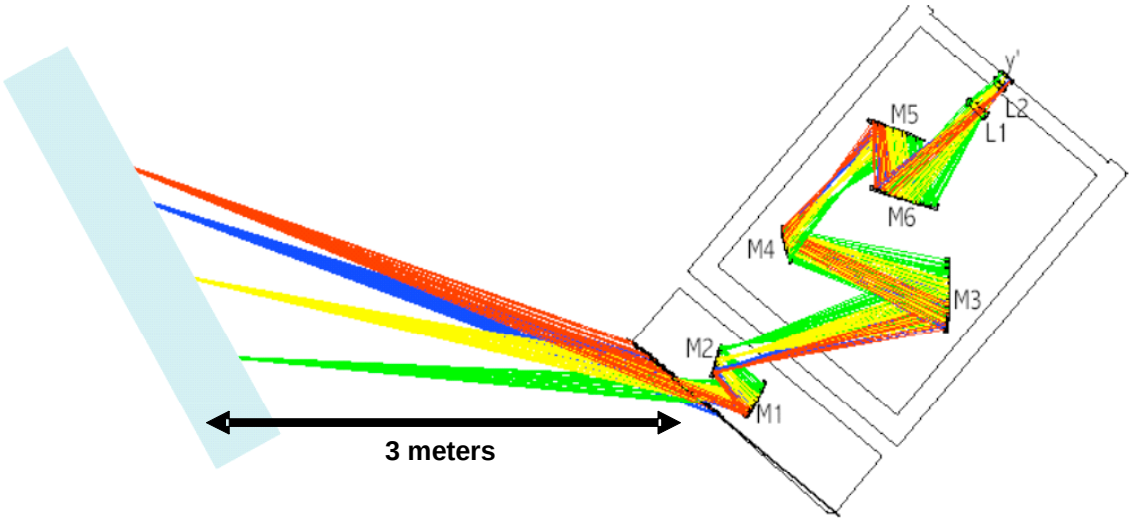

Figure 2-1. Existing ITER optical design for the edge MSE system. (called “EU” design)

Shown in Figure 2-1. is the ZEMAX model of the EU design. Only slight changes were required to the file supplied by the USIPO so that it was consistent with the current version of ZEMAX. The “EU” design utilizes six mirrors and one quartz lens to image light from neutral beam space to the image plane. The shape of the optical labyrinth was driven by the need for neutron shielding and the desire to keep the angle of incidence

small on each mirror. The supplied ZEMAX model used “default” parameters for the mirrors, so the code assumes that they are normal aluminum mirrors.

Mirror Sizes and Shapes

	Diameter	Shape
M1	270mm	Conic
M2	330mm	Plano
M3	600mm	Conic
M4	230mm	Conic
M5	535mm	Conic
M6	470mm	Conic
L1	140mm	Conic

Spot Radius in Neutral Beam Space in mm

Field	European
Top	66.9
Middle	75.2
Bottom	57.2

Polarization St. Dev. Across Pupil in Degrees

Field	European
Top	0.42
Middle	0.62
Bottom	0.79

Table 2-1(top) Mirror sizes and shapes of the EU design Table 2-2(middle), Image Spot Size (mm) at Three Locations in the Optical Plane, Table 2-3(bottom), Polarization standard deviation (degrees) across pupil

Shown in the Table 2-1. are the mirror sizes and shapes for the EU design. The mirrors are relatively large, which can drive up the cost. The shapes are fairly simple, which reduces the cost. Shown in Table 2-2. Are the image spot sizes in mm at three locations in the optical plane. Finally, in Table 2-3 is the polarization standard deviation (degrees) across the pupil. We had some concern about the quartz lens, as there would be

substantial Faraday rotation in this optic, and it is close enough to the plasma that it would be in a ~5T magnetic field.

Our next step was to determine how this optical design fit into the equatorial port 3 (eport 3), so the coordinates of the optical components were exported to a Pro-Engineer CAD file via a IGES file. This model is shown in Fig 2-2.

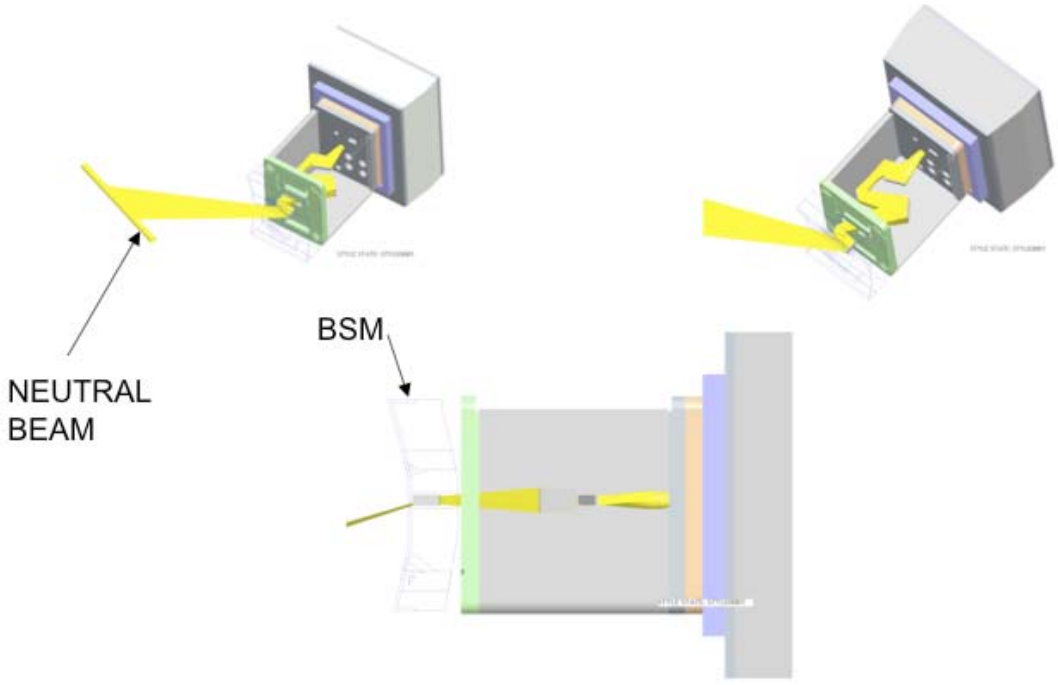

Figure 2-2. A Pro-Engineer CAD layout of the EU design for the edge MSE system

While the coordinates of the ZEMAX optical layout were close to those of the Pro-Engineer CAD model, they did not match exactly. Specifically, the first mirror location and angle did not allow a view of the neutral beam. We could not determine if the original CATIA model (which was converted to ProEngineer) had been slightly modified after the original ZEMAX design was completed. Some of the confusion also stems from the fact that the origin of the coordinate system for the CATIA and

ProEngineer CAD files is the center of the tokamak; it is very difficult to use this same origin for the ZEMAX file. We used a coordinate transformation to connect the two coordinate systems, and this is documented on the ProEngineer file. We were able to make slight modifications to the optical design, as shown in Figure 2-3, so that the optics fit into the port plug and the first mirror was directed at the middle of the neutral beam.

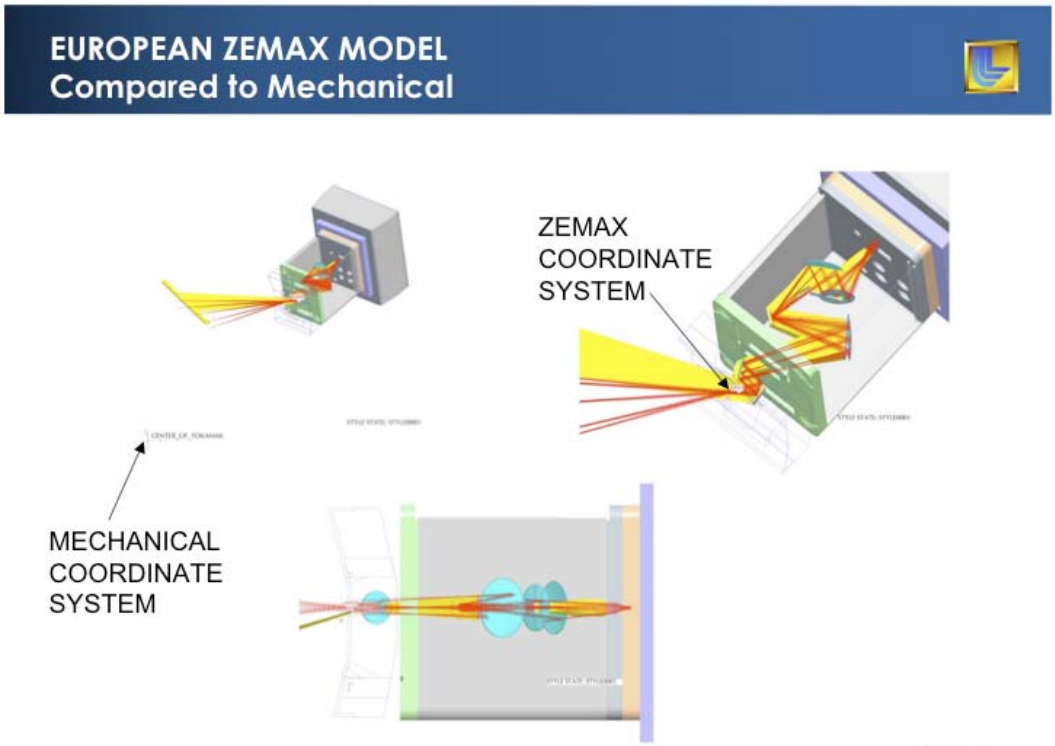

Figure 2-3. The EU ZEMAX model compared with the CATIA-ProE model. Note that the first mirror does not point towards the neutral beam. A simple coordinate transformation was used to connect the CAD model (origin at the center of the tokamak) with the ZEMAX (near first mirror)

In summary, after some effort, we were able to reconstruct the "EU" ZEMAX model and connect it with the CAD model. The optical performance of this system served as a reference for other designs. This effort completed this particular part of the SOW.

References for Section 2

2-1. Malaquias, A, et al., "Active Beam Spectroscopy Diagnostics for ITER", Rev. Sci. Instrum., 75 p 3393.

Section 3 Using relevant spatial constraints also provided by the Team Leader, explore alternate relay models and compare to the reference model with regard to the optical throughput and the polarization mixing.

The next step was to use the "EU" design described above and to explore other optical relay models. The SOW indicated two figures of merit- optical throughput and polarization preservation. In addition, we examined other constraints considered in the EU model; some of these are addressed in Ref. 3-1 and are summarized in Fig. 3-1.

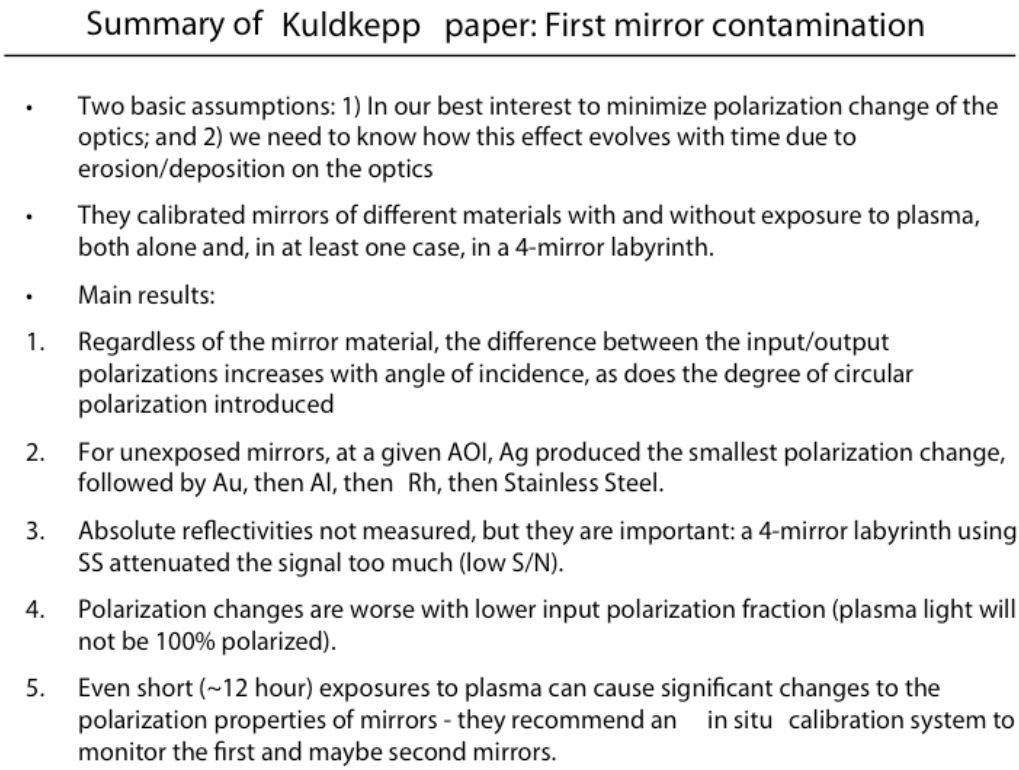

Fig. 3-1. Polarization design constraints from Kuldkepp paper

The paper outlines measurements of a 4-mirror system and the figure of merit is the "rotation angle" of polarized light. This is the change in the angle that the optical system introduces if there is an input of purely linearly polarized light. This is a good starting place, but while it is good to minimize any changes in polarization by the optics, if the change is relatively constant, it can be calibrated out. The Kuldkepp results drive

the design towards gold mirrors with a minimum angle of incidence, along with fewer mirrors. In the present design study, we also used other figures of merit available from ZEMAX to provide an optimum design. In addition, the neutron shielding requirement sets the number and shape of bends in the optical train in the port plug.

For this work, we established the following desireable optical characteristics:

1. Minimize the affect on the polarization state of the incoming light, particularly if this varied widely over the field of view. For this study we used ZEMAX, but we would like to use measured Meuller matrices of typical mirrors in an optical ray tracing code in future studies of polarization response.
2. Minimize the number of mirrors, subject to the constraint of sufficient neutron shielding.
3. The first two mirrors closest to the plasma would be metal mirrors (i.e. non-ideal from the standpoint of polarization), and the remaining mirrors would be dielectric mirrors (nearly ideal).

Both the optical designer that worked on this project (S. Lerner) and the optical designer that built the MSE system on DIII-D and worked on the ITER IRTV optical design (L. Seppalla) have also adopted a very useful design form, as shown in Fig. 3-2.

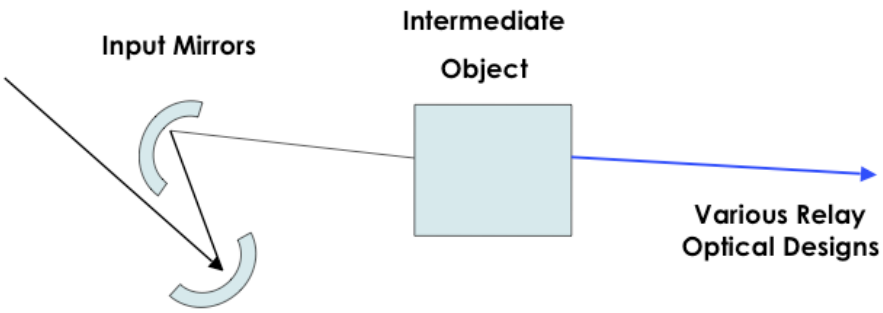

Fig. 3-2 Intermediate Object Optical Design Concept

The two input mirrors, which are metal, are used to form an intermediate object. Then the optical designer can relay this object to the input of the polarization analyzer with a

variety of more or less “standard” optical designs. In the ITER IRTV design, a Cassegrain telescope was used in the relay chain. In the present design for MSE, several design forms were explored, as shown in Fig. 3-3.

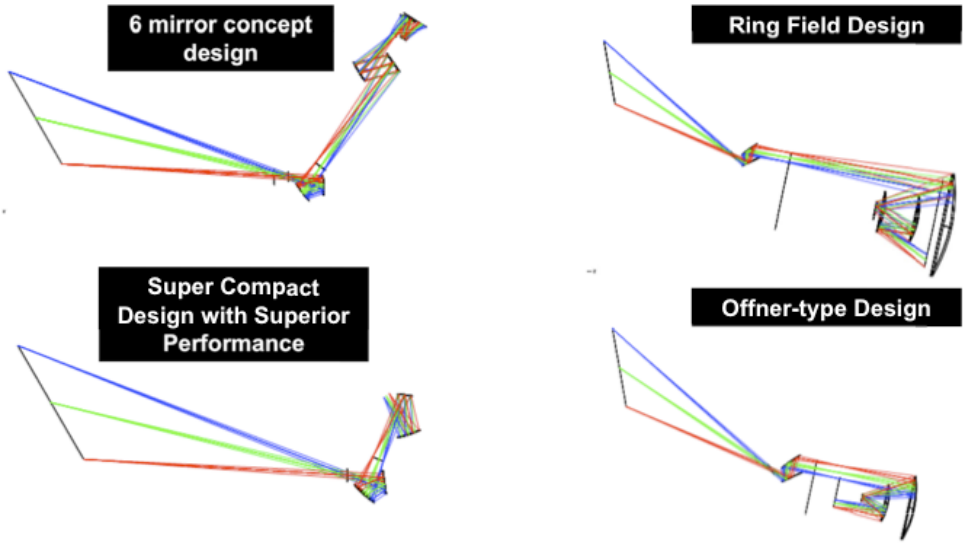

Fig. 3-3 Typical optical relay designs that were explored

After exploring this variety of design forms, the first design that was examined in detail was LLNL-1, as shown in Fig. 3-4. The LLNL-1 design uses four mirrors and a

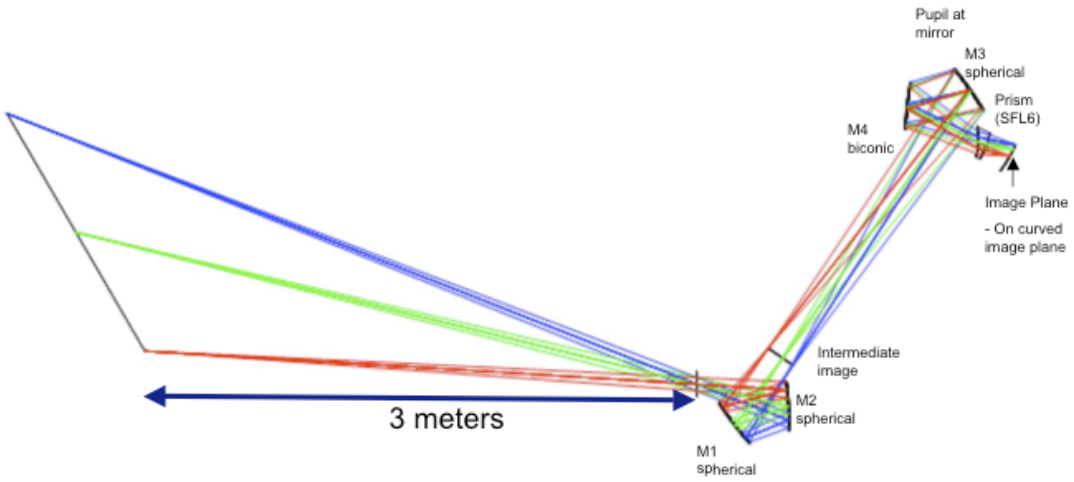

Fig. 3-4 Optical Design LLNL-1

SLF_6 prism to transfer the light from the neutral beam interaction region to the input of the polarization analyzer. The special prism has very low Faraday rotation, and we have verified that this can be manufactured in the size required by the design. The relatively small angles of incidence of the mirrors lead to relatively small polarization aberrations. The design also has smaller mirror sizes and therefore less estimated cost compared to the EU design. The details of the LLNL-1 design are shown in Fig. 3-5.

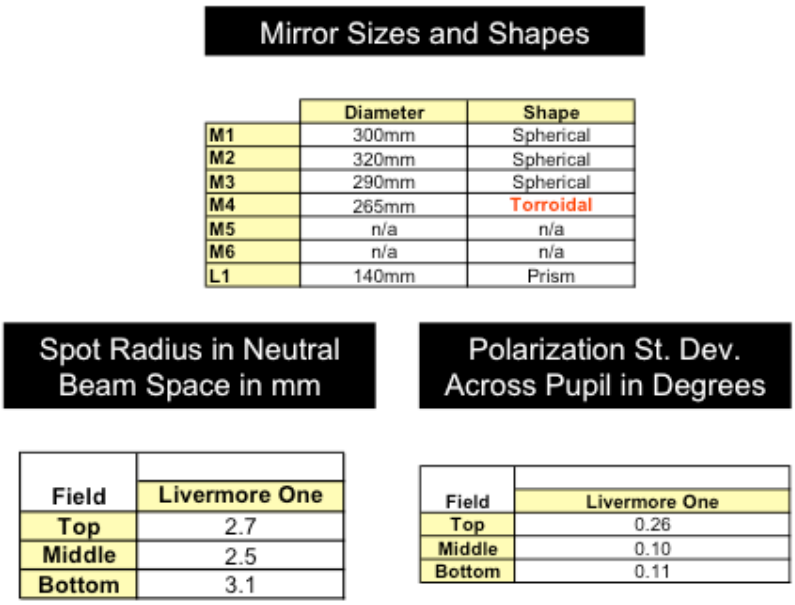

Fig. 3-5 Details of the of Optical Design LLNL-1. The spot radius has been reduced by over an order of magnitude compared to the EU design, the polarization aberration has been reduced by a factor of 3, and the sizes of the mirrors have been reduced. The toroidal optic would be the most expensive to fabricate.

The LLNL-1 design compared with the EU design:

- Reduced the spot radius by over an order of magnitude
- Reduced the size and number of mirrors
- Reduced the polarization aberration by about a factor of 3
- Had one complicated shape (toroidal), with small angles of incidence

However, when the ZEMAX model was exported to the ProEngineer CAD model, we found that it required the polarization analyzer to be in the port plug, or

additional optics would be required to relay the image out of the port plug. Fig. 3-6 shows an overlay of the EU design with the LLNL-1 design.

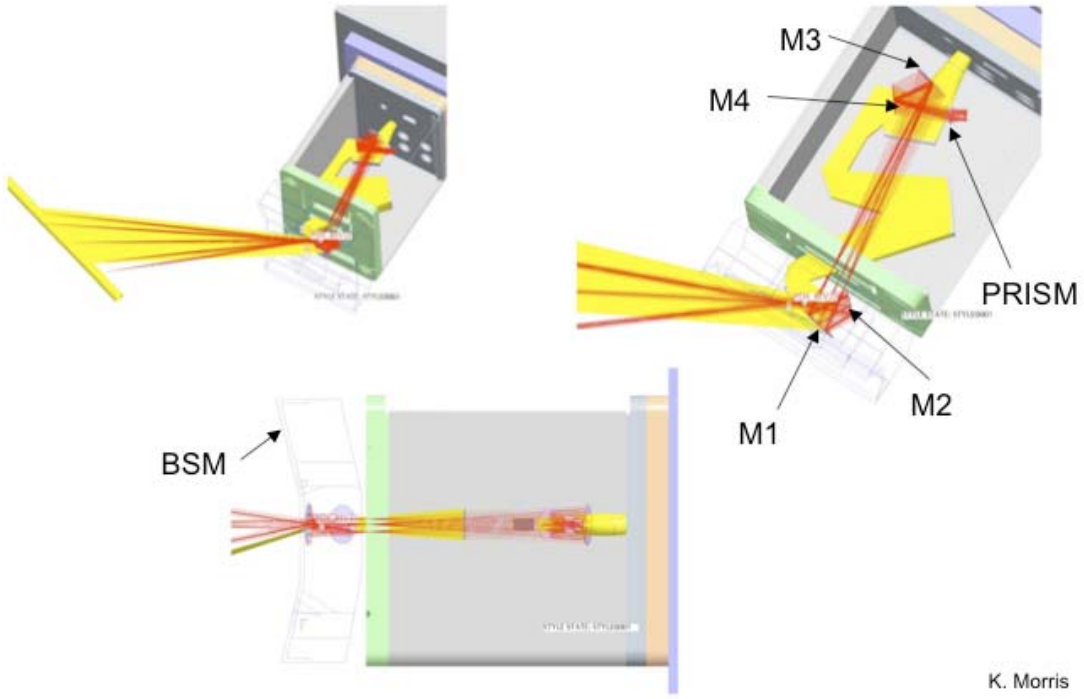

Fig. 3-6 The LLNL-1 design (red) overlayed with the EU design(yellow). Note that the prism and the polarization analyzer of the LLNL-1 design are located in the port plug.

Discussion with the USIPO (two video conference calls were held which were extremely helpful to the MSE team) led us to develop two more design constraints:

- The optics should relay the image out of the port plug, so that the vacuum window was in the back wall of the port plug
- The first two mirrors should be as far away as possible from the plasma, but the opening in the blanket shield module (front end) should be as small as possible, and should not extend into the walls of the port plug.

Further iteration between the USIPO staff, the ProEngineer CAD model, and the ZEMAX optical model resulted in an improved design called LLNL-4B, as shown in Fig. 3-7. This design uses four mirrors and one SLF_6 lens in the image train.

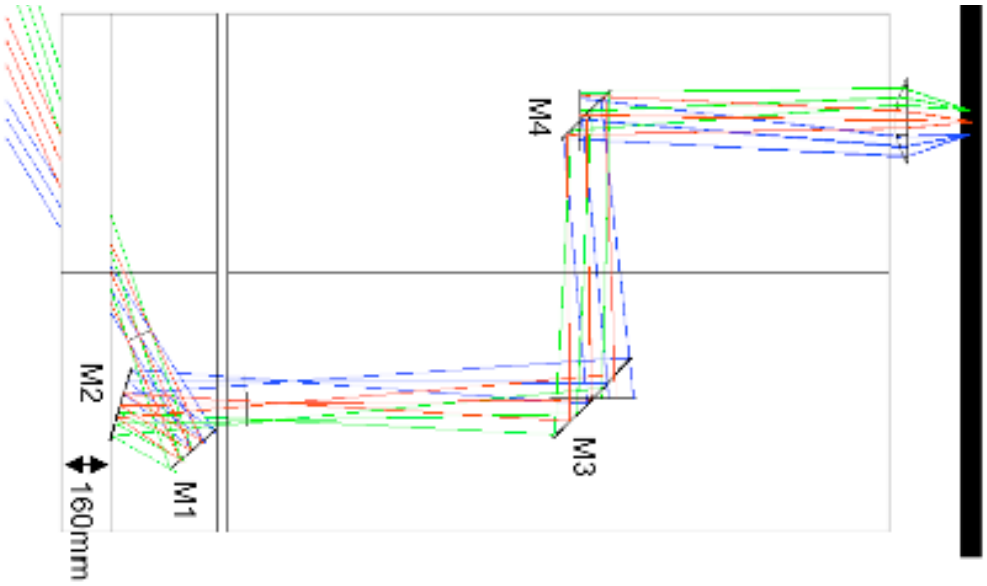

- M2-port plug clearance: 160mm minus mirror thickness
- Field width 100mm

Fig. 3-7 The LLNL-4B design – this is the most optimized design at the end of the study

Mirror Sizes and Shapes

	Diameter	Shape
M1	205mm	Spherical
M2	230mm	Cylinder
M3	420mm	Spherical
M4	250mm	Anamorphic
M5	n/a	n/a
M6	n/a	n/a
L1	200mm	Spherical

Spot Radius in Neutral Beam Space in mm

Field	Livermore Four
Top	6.0mm
Middle	6.5mm
Bottom	7.8mm

Polarization St. Dev. Across Pupil in Degrees

Field	Livermore Four
Top	0.07
Middle	0.14
Bottom	0.20

Fig. 3-8 The LLNL-4 design – this is the most optimized design at the end of the study

The Livermore 4b design takes into account all of the above figures of merit. As discussed above, the angles of incidence of the light on the mirrors is minimized to minimize the polarization errors. Furthermore, metal mirrors (M1 and M2) typically have larger polarization errors compared to carefully coated dielectric mirrors. Thus, minimizing polarization errors from metal mirrors M1 and M2 should be more critical than the polarization errors from dielectric mirrors M3 and M4. Therefore, mirrors M1 and M2 are oriented as to minimize the angles of the incident light and mirrors M3 and M4 have their orientation defined by the neutronics shielding requirements.

In defining the stop location we trade-off both the beam footprint on the port plug face and the size of mirror M1. Locating the stop at the port plug face minimizes the port plug face beam footprint and locating the stop at mirror M1 minimizes the size of mirror M1. Limiting the size of M1 to approximately 8" then defines the stop location.

The figure and angles of mirrors M1 and M2 are then optimized. Mirror M1 is spherical and mirror M2 is cylindrical. We then optimize the figures, locations, and orientations of M1/M2 with the constraints that M1 and M2 form a relatively well corrected intermediate image, that M1 and M2 fit within the geometric boundaries of the port plug, that M2 be small, that Mirror M3 be relatively small, and that the light propagates roughly perpendicular to the port plug face.

Mirrors M3, M4, and lens L1 then relay the intermediate image to a position outside and perpendicular to the back boundary of the drawer. The orientation and locations of mirrors M3 and M4 are defined by the neutronics (shielding) requirements. L1 is located outside the back surface of the drawer – again for neutronics consideration. Optical glass SFL_6 is chosen for lens L1 as it has a low Verdet constant. Mirror M3 is

spherical and mirror M4 is an anamorphic asphere. The anamorphic asphere shape of mirror M4 can be used to effectively correct for the residual optical aberrations of the first three mirrors in the system. We then optimize the surface figure of M3/M4/L1 with the constraints that we minimize the size of M4 and L1, and that we have acceptable image quality.

The large number and stringency of the system requirements narrowly define the optical layout. While there is some room to optimize the design within the current constraints, a significant improvement of the design would require a significant redefinition of the constraints (such as the neutron shielding or optical spot size).

The next step was to examine in more detail how well the LLNL design fit into the port plug. This is shown in a series of figures that are outputs of the ProEngineer CAD model. Fig. 3-9 is a view from the inside of the tokamak looking out to show the face of the port plug. Fig. 3-10 is a top view that shows the relationship between the first mirror (M1) and the face of the blanket shield module.

It should be noted that there was a change between the LLNL-4 and LLNL-4B designs. The setback of M1 from the plasma was increased from 100mm to 160mm in going from the LLNL-4 to the LLNL-4B designs. The extra setback was recommended in a second conference call with the USIPO. In addition, it was desirable to have this mirror and mount have minimum mass, as they are closet to the plasma.

Figure 3-11 compares the sizes of the optical elements for the EU, LLNL-1, and LLNL-4 designs. Figure 3-12 compares the polarization rotation and the polarization standard deviation across the pupil as calculated by ZEMAX. This calculation assumes

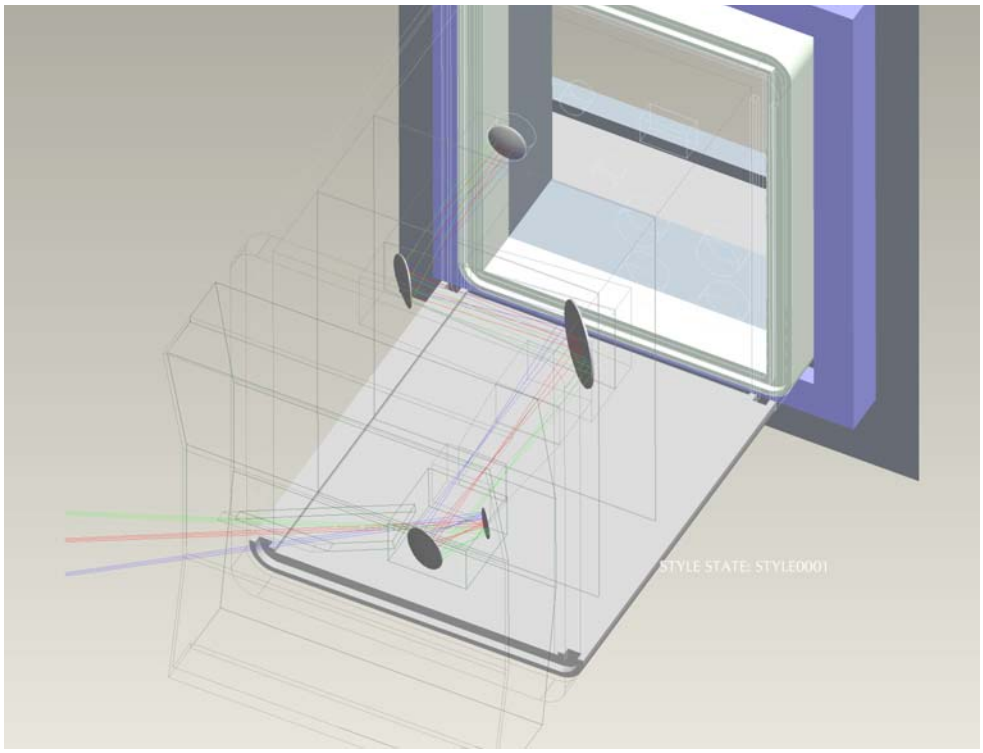

Fig. 3-9 ProEngineer model of the LLNL-4 design for the edge MSE system.

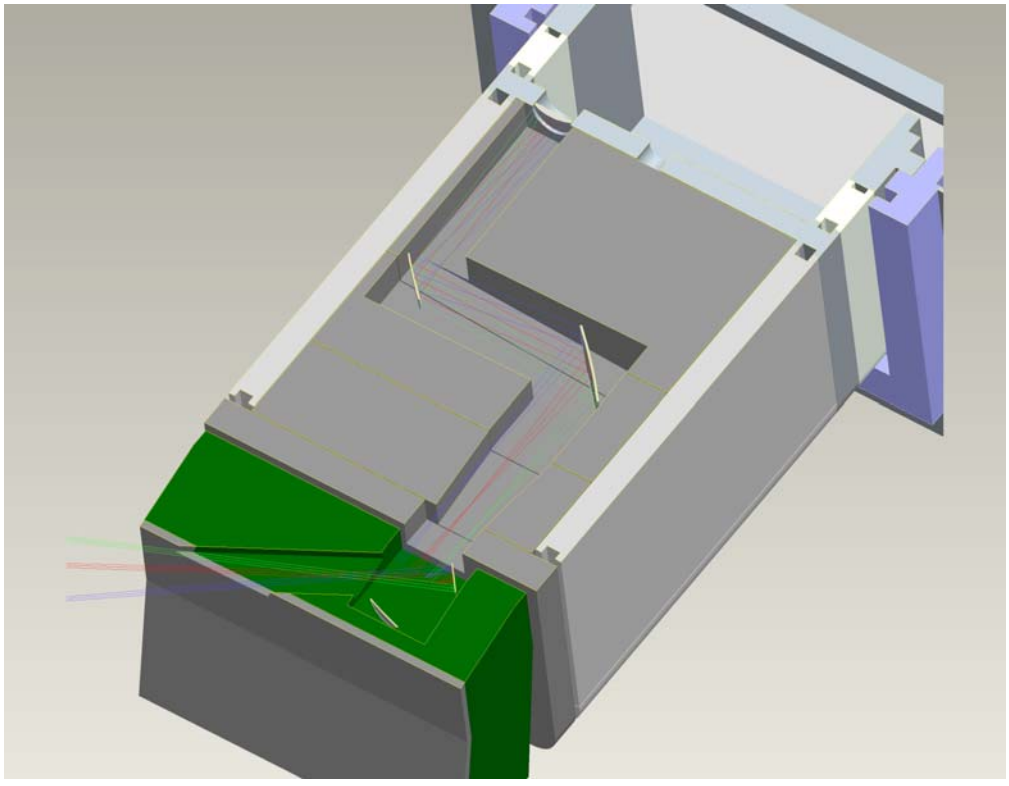

Fig. 3-10 ProEngineer model of the LLNL-4 design (top view).

that only the first two mirrors, made of aluminum, make a significant contribution to polarization aberrations.

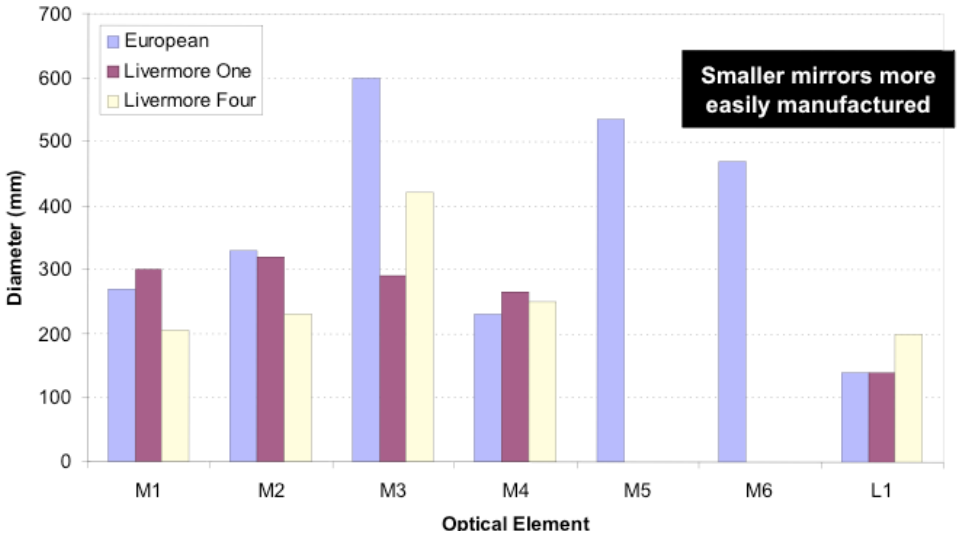

Fig. 3-11 Sizes of the mirrors for the EU, LLNL-1 and LLNL-4 designs

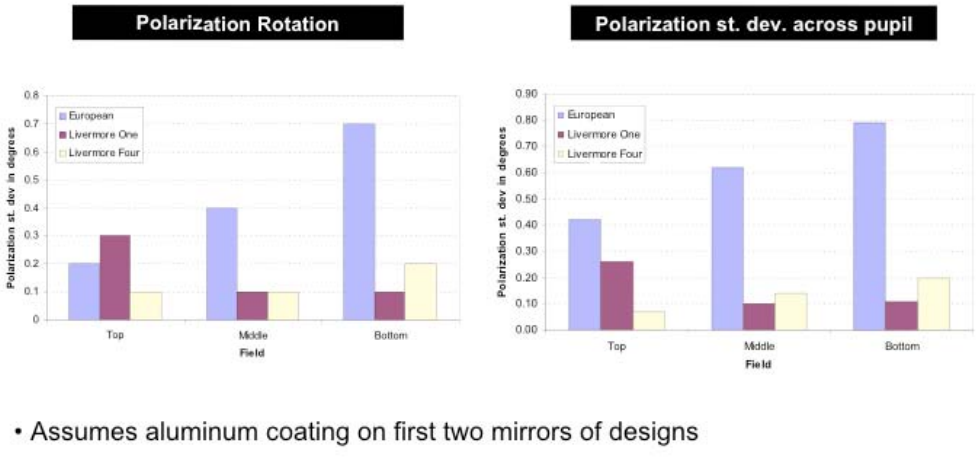

Fig. 3-12 Sizes of the mirrors for the EU, LLNL-1 and LLNL-4 designs

Related to the size of the optics in Fig. 3-11 is the relative cost of the three optical designs. To obtain a quick estimate of the cost, we assumed that:

- Cost was proportional to the square of the element area
- Cylindrical elements were 2X the cost of spherical elements
- Aspheric elements were 2X the cost of spherical elements
- Anamorphic elements were 4x the cost of spherical elements

Using these assumptions, we obtain:

- EU relative cost = 100%
- LLNL-1 = 20%
- LLNL-3 = 30%

In addition, the beam footprint at M1 and M2, as shown in Fig. 3-13 is rectangular, so the mirror can also rectangular. This cuts down on the size and mass of the optic that is close to the plasma.

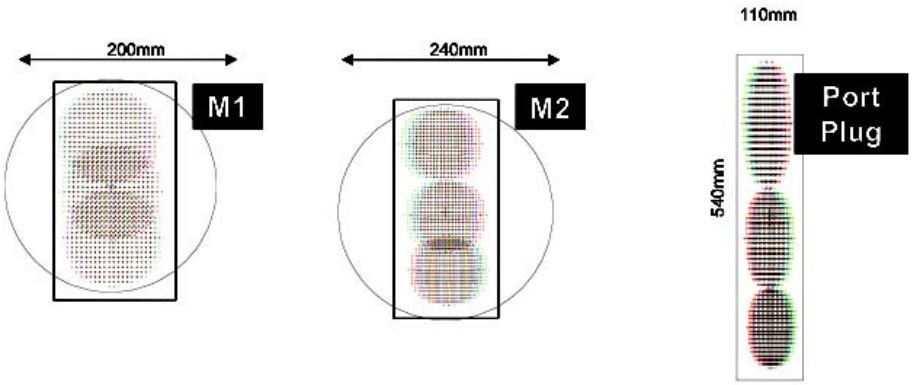

Fig. 3-13 Beam footprint at M1, M2, and the Port Plug – rectangular optics can be used

Figure 3-13 shows the relative imaging performance of the designs, the LLNL-4B design has roughly an order of magnitude better performance than the EU, and about ½ that of LLNL-1. Some loss in optical performance has been sacrificed to meet the other requirements of fitting in the port plug, and the first mirror needs to be moved back from the plasma.

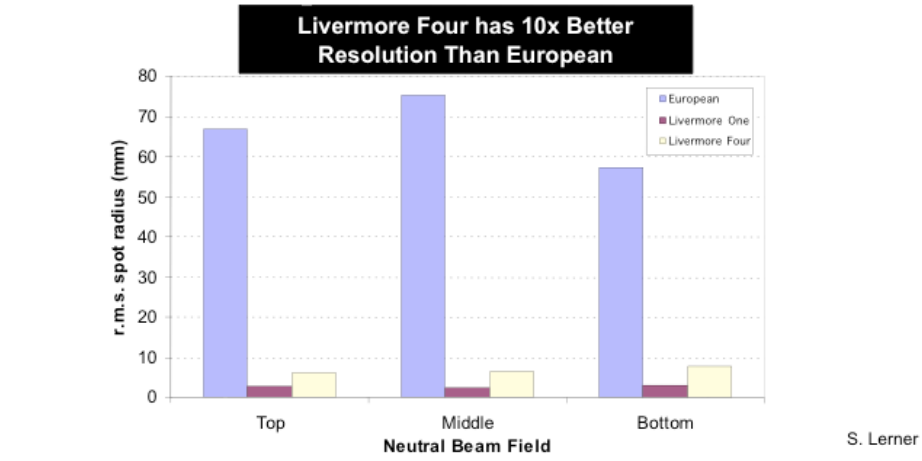

Field	European	Livermore One	Livermore Four
Top	66.9	2.7	6
Middle	75.2	2.5	6.5
Bottom	57.2	3.1	7.8

in mm

Fig. 3-14 Imaging performance of the three designs is compared. LLNL-4 has slightly degraded performance but matches the port geometry and other constraints.

Section 4 Model the transformation of the polarization state of an appropriate plane labyrinth and conduct laboratory polarimetry experiments to test this model.

The next three figures 4-1(EU), 4-2(LLNL-1), and 4-3(LLNL-4B) examine in detail the polarization performance of the three designs. In each case, a polarization map is provided at the top, middle, and bottom of the field. Again, this assumes that only the first two aluminum mirrors have polarization aberrations and contribute to the polarization errors.

Some preliminary work was also done to assess the polarization performance of first mirrors made of other materials. These were modeled by using a complex index of refraction for the metal coating. A value of n=0.82 = 5.99i at 546nm was used for Al.

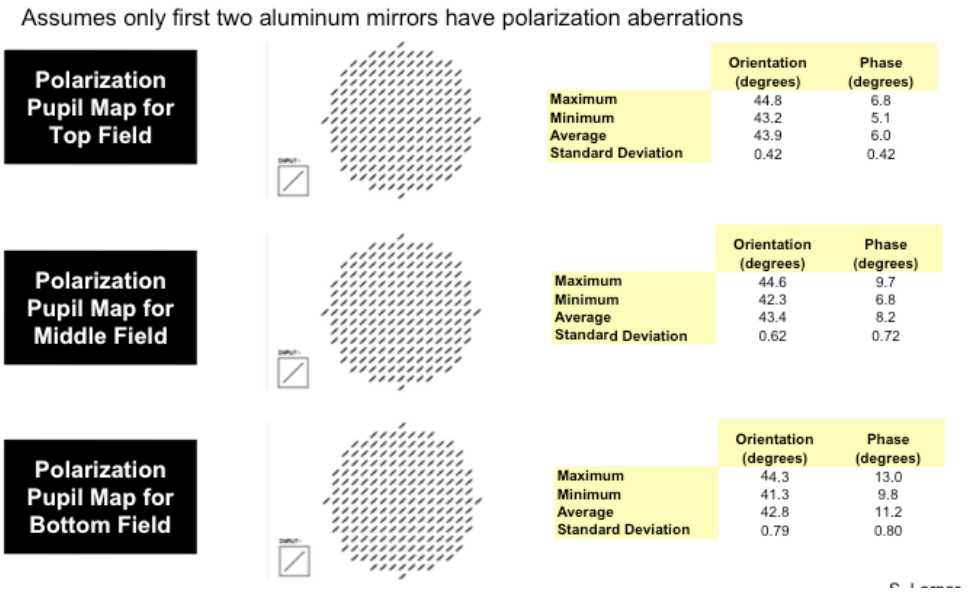

Fig. 4-1 Detailed polarization performance of the EU design, with first two Al mirrors

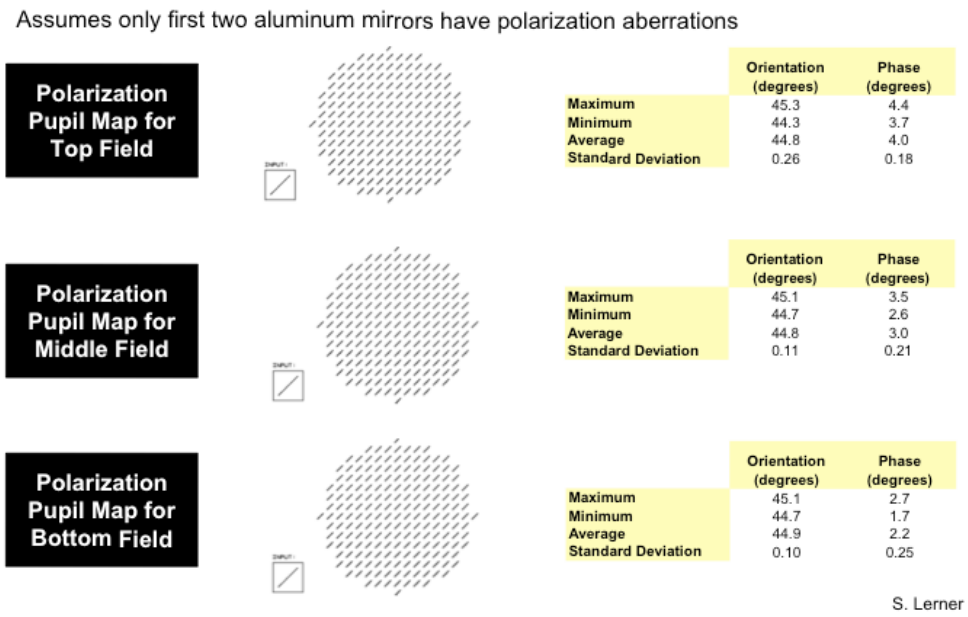

Fig. 4-2 Detailed polarization performance of the LLNL-1 design, with first two Al mirrors

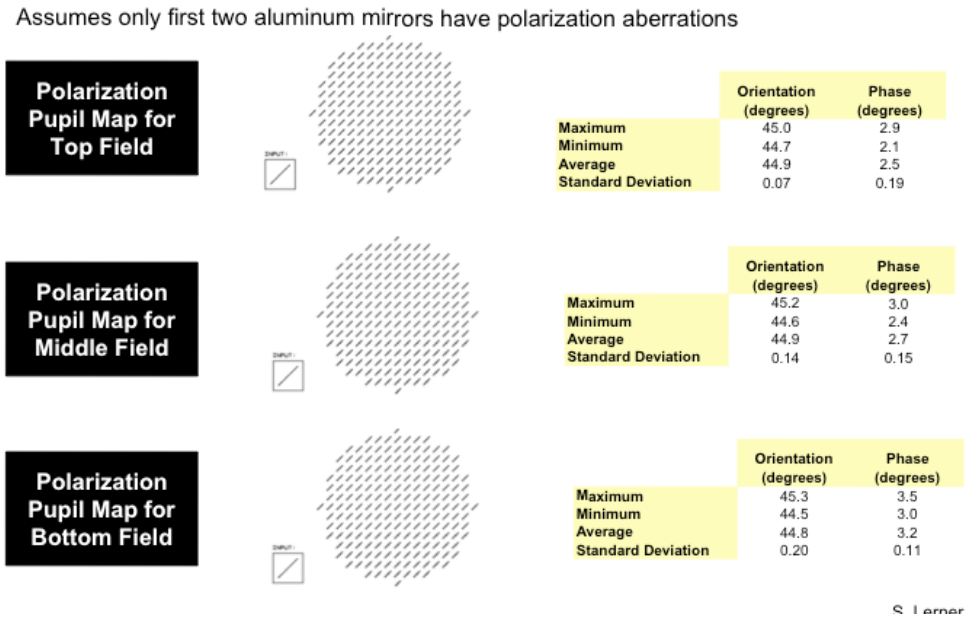

Fig. 4-3 Detailed polarization performance of the LLNL-4 design, with first two Al mirrors

Calculations were also performed for gold (n=5.966 – 39.1 i at 650nm) and Rhodium (n = 2.2 – 5.75 i at 653 nm). The coating was assumed to be uniform. These results are shown in Fig. 3-17.

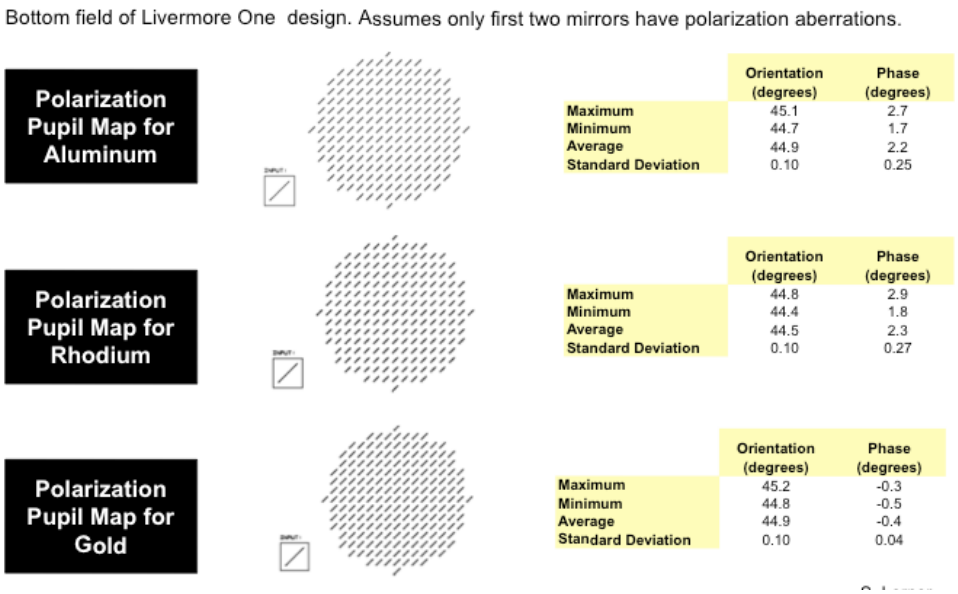

Fig. 4-4 Comparison of (modeled) aluminum, gold and Rhodium mirrors

We have obtained measurements of an “ideal” dielectric mirror, and these are included in the section on calibration. We were not able to complete full Mueller matrix measurements of metal mirrors during the contract period.

Section 5 Core MSE system analysis

After the design of the edge system was mature, we used a similar design form for the core system. This system sits higher in the equatorial port so that it can look over one

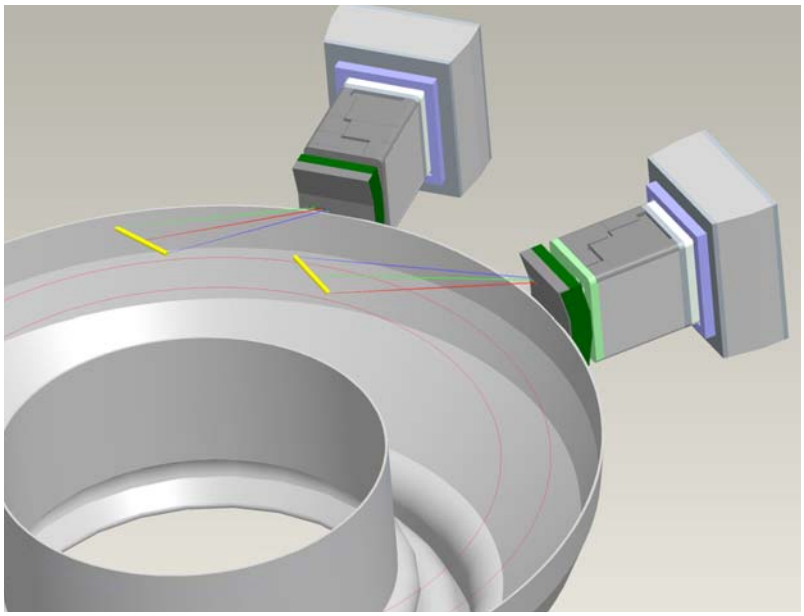

Fig. 5-1 Layout of edge (port3) and core(port1) systems

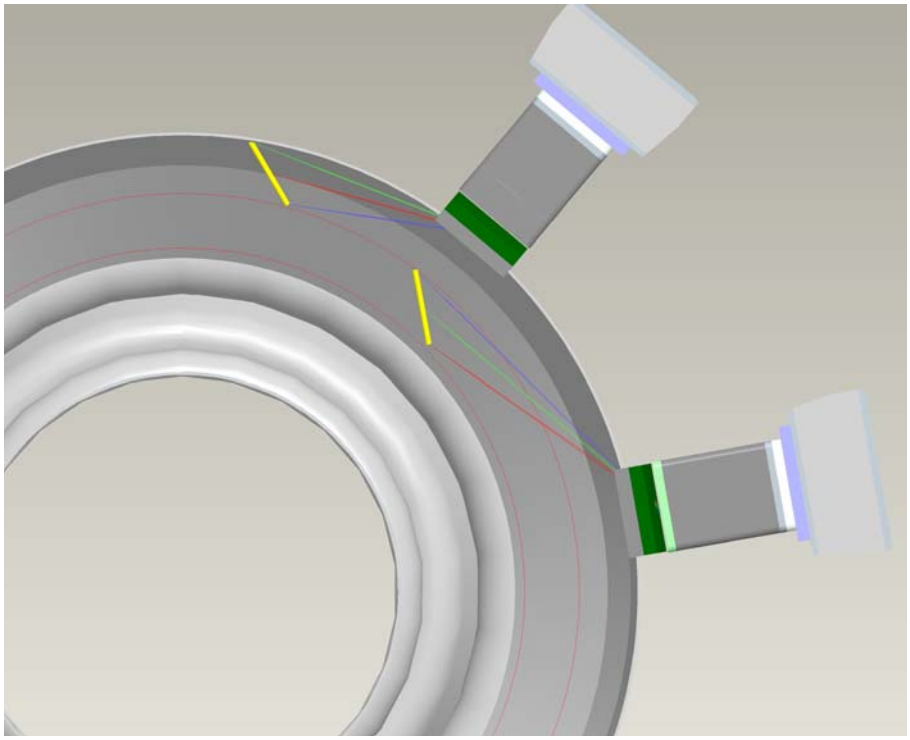

Fig. 5-2 Top view of edge (port3) and core(port1) systems

of the neutral beams and thereby minimize it's interference. A ProEngineer CAD layout

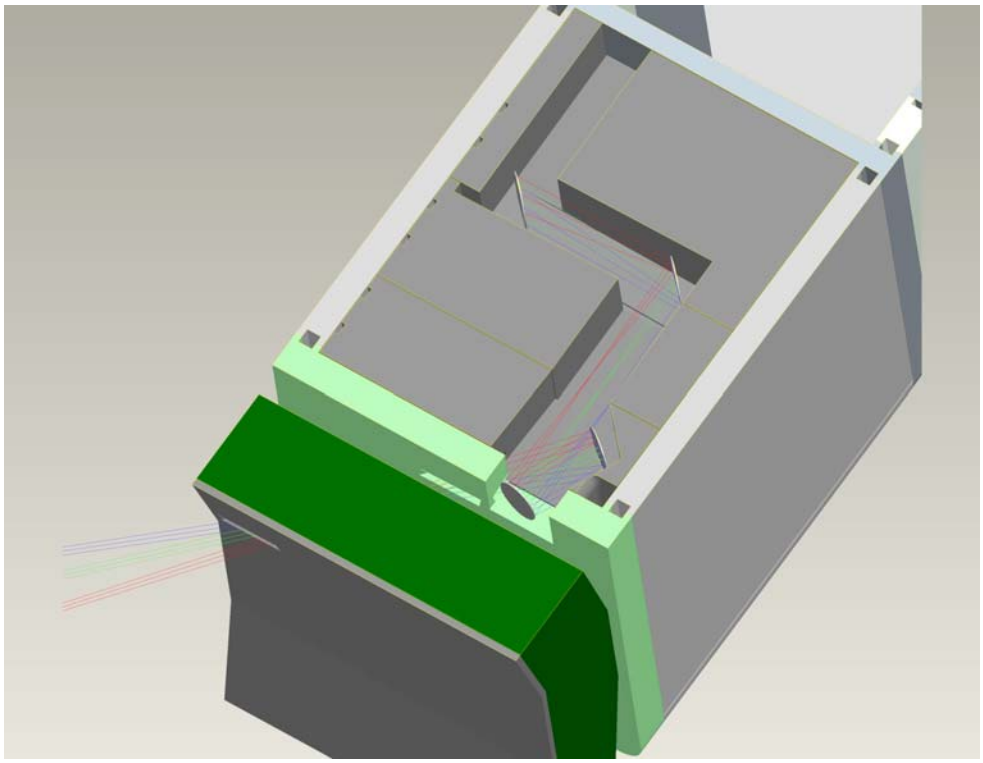

Fig. 5-3 Layout of core MSE system, using a similar design form as for the edge system

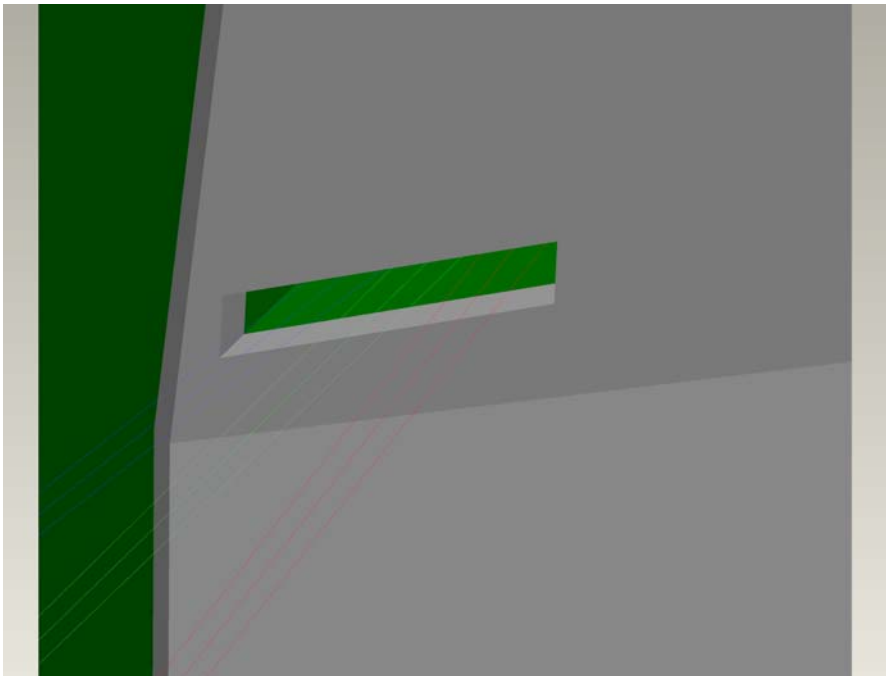

Fig. 5-4 Closeup of the penetration in the blanket shield module for the core system

of both ports are shown in Figs. 5-1, 5-2, and 5-3.

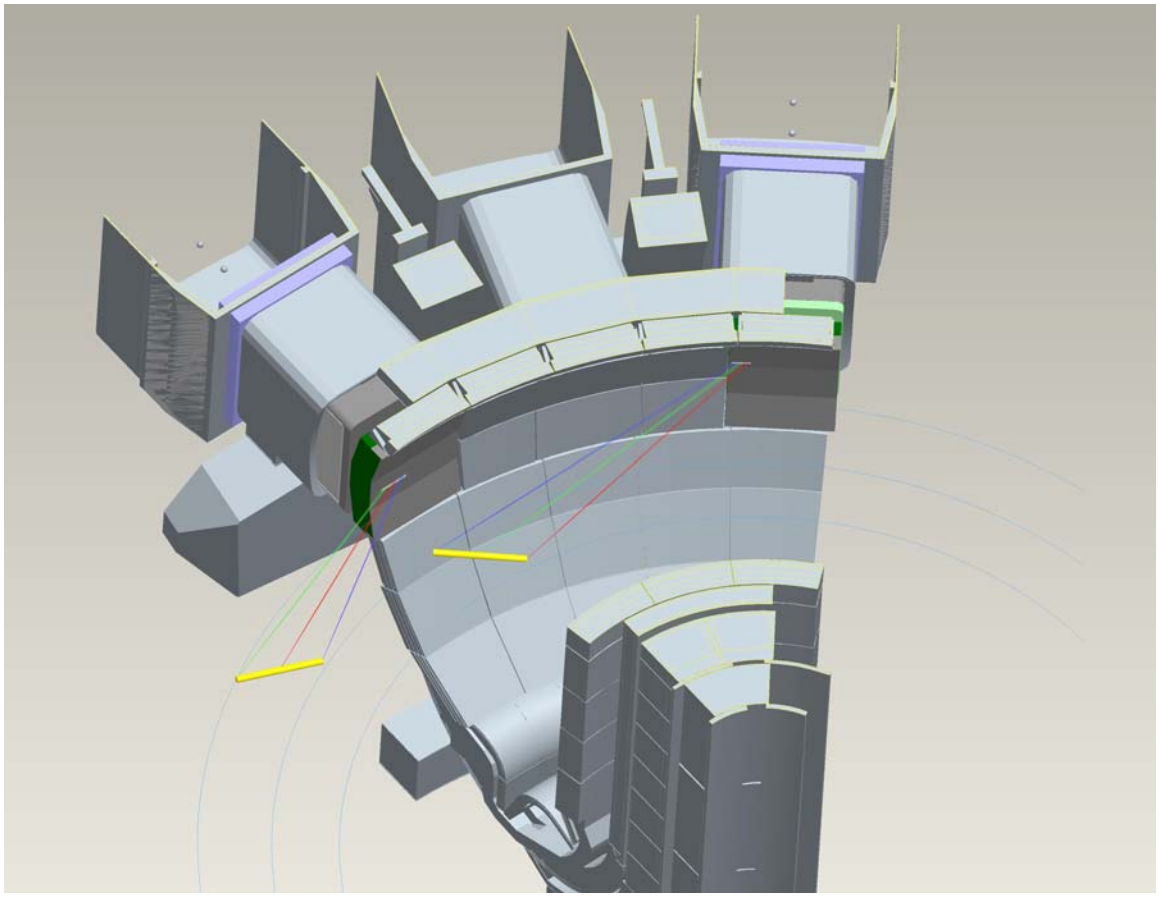

Fig. 5-3 Layout of the core and edge MSE optical designs

In the detailed optical design, we were able to move the first mirror M1 farther back from the plasma so that it was not in the Blanket Shield Module. We would expect that M2, and most likely M1 would then be far enough removed from the plasma that dielectric (nearly perfect from the polarization standpoint) mirrors could be used. Shown in Fig. 5-4 is the LLNL Core MSE design. It uses four mirrors and one SLF_6 mirror to relay the light to the polarization analyzer. As shown in Fig. 5-5, two of the mirrors are anamorphic in shape and thus would be slightly more expensive; about 35% of the EU compared to the 30% of the LLNL-4 edge system. The spot radius is a little larger than

Layout of Livermore Core Design

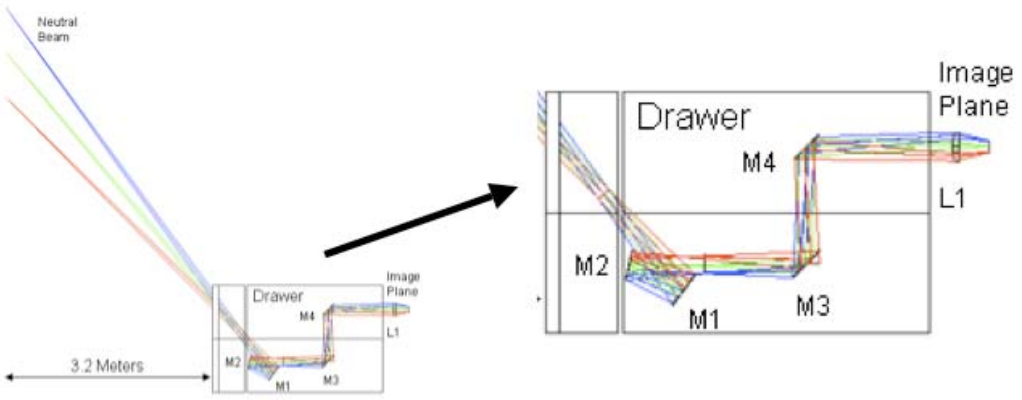

Fig. 5-4 LLNL Core MSE Optical Design

Mirror Sizes and Shapes

	Diameter	Shape
M1	270mm	Anamorphic
M2	200mm	Spherical
M3	250mm	Spherical
M4	250mm	Anamorphic
M5	n/a	n/a
M6	n/a	n/a
L1	200mm	Conic

Spot Radius in Neutral Beam Space in mm

Field	CORE
Top	13
Middle	10
Bottom	16

Polarization St. Dev. Across Pupil in Degrees

It should be possible to coat all mirrors with a dielectric coating that does not introduce significant polarization aberrations. **In that case the polarization aberrations will be close to zero.** If a metal coating is needed, the polarization aberrations will be similar to the LLNL-4 design.

Fig. 5-4 Details of Core MSE optical design

the edge system, but certainly within specifications. If M1 and M2 are sufficiently removed from the plasma, we may be able to use dielectric mirrors for this system, which will dramatically reduce the polarization aberrations in the system.

We summarize the imaging performance of all the systems in Fig. 5-5, and the mirror sizes are compared in Figure 5-6. Finally, in Fig. 5-7, the light footprint at M1, M2 and the port plug is shown. Note the somewhat asymmetrical pattern on M2. This is indicative that the anamorphic shapes of M1 and M3 are "fighting" each other (having to correct each other), which could be reduced by further optimization studies.

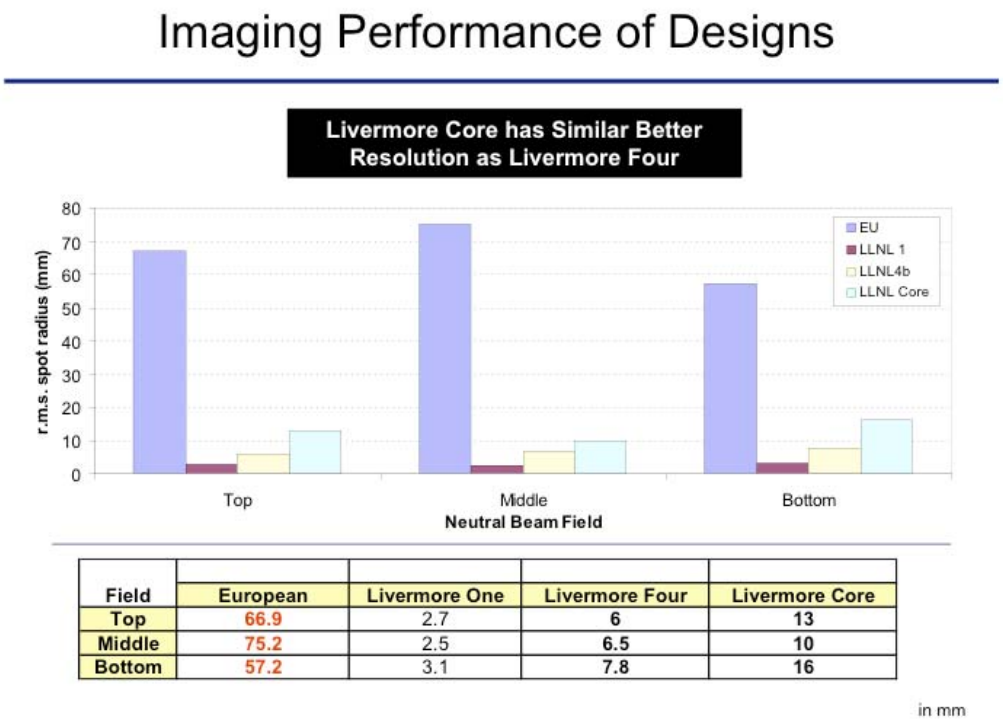

Field	European	Livermore One	Livermore Four	Livermore Core
Top	66.9	2.7	6	13
Middle	75.2	2.5	6.5	10
Bottom	57.2	3.1	7.8	16

Fig. 5-5 Comparison of beam spot size in all the designs

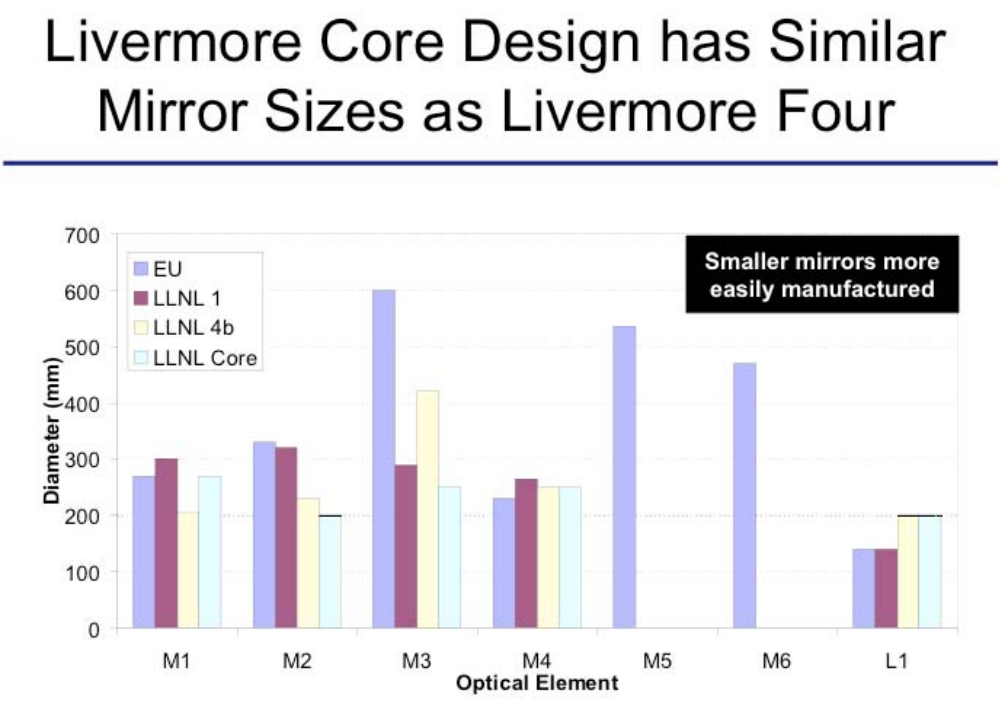

Fig. 5-6 Comparison of mirror sizes in all the designs

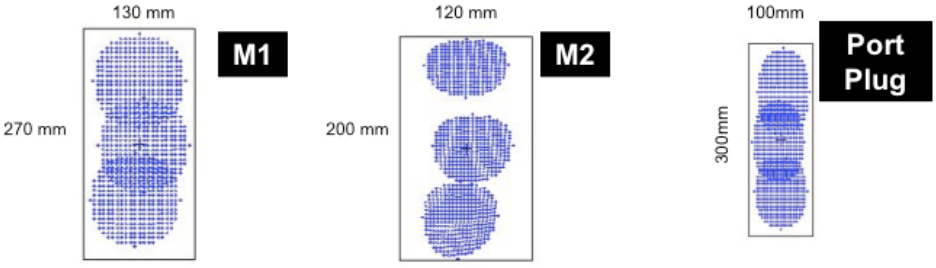

Fig. 5-7 Beam footprint at three locations in the core design

6. **Section 6** Develop a concept for an in-situ calibration scheme capable of characterizing the effects of the mirror labyrinth on the polarization state of the light collected from each of the radial positions where MSE measurements are sampled.

This section deals with various in-situ calibration schemes that are capable of characterizing the effects of the optical system on the collected polarization. Each subsection is a self-contained summary or report of a particular technique. The first describes the “traditional”, basic calibration procedure used presently on the DIII-D MSE diagnostics. This is followed by a more lengthy report on calibration using the beam into gas technique, including a discussion of various anomalies observed using this on DIII-D and likely explanations. The next subsection describes a new in-situ calibration technique still under investigation that treats elliptical polarization more completely and offers a way to determine the system Mueller (i.e. linear transfer) matrix. Finally, the last subsection speculates about possible instrumentation that could be built into the diagnostic for between and during shot calibration monitoring.

6.1 In-Situ MSE calibration using linear polarizers placed in the vessel at air

The basic calibration procedure for MSE on DIII-D could be a starting point for MSE on ITER. It requires an at air vessel entry. A rigid support structure is placed in the vessel that holds and levels an optical rail aligned with the neutral beam. (This structure is also used for recording the spatial location of each channel). A large diameter (6") linear polarizer is mounted to an Oriel 6" clear aperture precision rotation stage. This is mounted on a lockable swivel post on a lab jack that slides along the optical rail. A large area light emitting paddle made of fiber optics bonded between plastic is mounted to the stage behind the polarizer. Individual channels are backlit to align the polarizer. This setup is shown in Figure 1. (Note that calibration scans are actually performed without room lights on).

Figure 1. Basic MSE calibration on DIII-D.

Control software steps the polarizer angle through 60° or more, and the signals $I(2\omega_1)$ and $I(2\omega_2)$ (intensity at the second harmonics of the PEMs) are recovered using lock-in amplifiers.

Modeling of the MSE optical components using Mueller matrices led to the introduction of a calibration fitting function known as the tangent-offset model. [Makowski, M.A. et al, "Improved signal analysis for motional Stark effect data", RSI, **76**, 023706

(2005)]. This function is an improvement over the previously used tangent-slope model (described in 6.2), and is:

$$\frac{I(2\omega_2)}{I(2\omega_1)} = \text{Gain} \cdot \tan\left(2\left(\gamma + \text{Phase} + B_{t\text{scale}} \cdot B_t\right)\right) + \text{DC offset},$$

where γ is the polarization azimuth. The parameters Gain, Phase, and DC offset are fit to the data collected in the in-vessel polarizer scan. These are sensitive to, and include the effects of the gains and offsets in the data acquisition system (i.e. signal amplifiers and lock-in amplifiers), as well as the present wavelength, retardation, and to a lesser degree, temperature settings of the PEMs.

The parameter $B_{tscale} \cdot B_t$ accounts for (toroidal field induced) Faraday rotation in the vacuum window and possibly other refractive optical elements. (While lenses are typically made from low Verdet SFL6 glass to avoid this problem, vacuum window manufacturers have told us that the high coefficient of thermal expansion of SFL6 would make it extremely difficult to make a glass to metal seal). Establishing B_{tscale} for each channel requires pulsing the toroidal field up to full strength with a fixed polarizer inside the vessel. Since personnel and "free floating" tools may not be permitted inside the machine hall, much less the vessel during a 2 Tesla field-only shot, using the single in-vessel polarizer to acquire B_{tscale} one channel at a time is infeasible due to time constraints. A different set up is used with stationary light sources and linear polarizers (Moxtek) aligned with all channels in an array at once. This is shown in Figure 2.

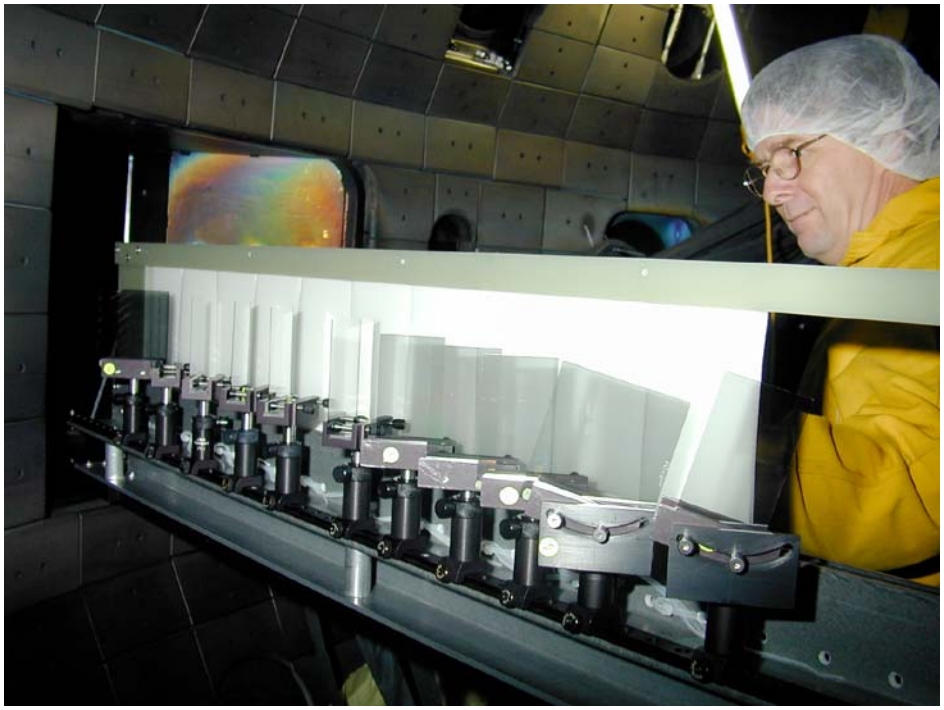

Figure 2. Light panels aligned with the beam and Moxtek polarizers for Btscale calibration.

Using the setup in Figure 2, the toroidal field may be scanned on successive shots to derive B_{tscale} for each channel. Care must be taken to break any conducting loops in the support structure holding the in-vessel polarizers to avoid any vibration from jxB forces.

Clearly, the extent to which personnel and material are allowed entry into the ITER vessel will determine the usefulness of these in-situ calibration techniques. If man-entry is limited/prohibited, it's conceivable that these techniques may be adapted to work using remote handling. It may not be necessary to station the in-vessel polarizers exactly at the focus of each channel at the beamline. As long as the source of polarized light fills the solid angle of each channel at some position in front of the first optic, the same procedures should work. In this case, it may be convenient to use remote handling to position polarizers directly in front of the port opening.

6.2 Calibration of Motional Stark Effect Diagnostic using the Beam in Gas technique:

6.2.1. Introduction

The Motional Stark Effect Diagnostic is the diagnostic of choice to measure internal magnetic field in hot plasma where the polarization components from energetic neutral particles can be observed. In particular, in Tokamaks with a strong toroidal field, the poloidal magnetic field and radial electric field can be measured [1-3] from the D-alpha spectrum emitted by a deuterium beam. There is now a crucial need for a full understanding of this diagnostic and the development of well established calibration techniques, since the diagnostic will be employed in ITER [4,5]. In this diagnostic, the spectral line is Stark split due to the Faraday electric field produced by the cross product of the beam neutral velocity and the magnetic field. The central 3 Stark components are polarized perpendicular to the electric field (sigma –σ) and the other 6 components are polarized parallel to the electric field (pi –π). (Figure 1). In a typical implementation of the system (Figure 2), the polarimetry involves a pair of photo-elastic modulators (PEM) which produce signals at two frequencies, one corresponding to the sine of twice the polarization angle and the other to the cosine of twice the polarization angle. The total light output from the PEM is filtered to select one polarization (sigma or pi) and is detected by a photomultiplier tube (PMT). The total intensity from the PEM is given by the expression

$$I \sim I_{bk} + I_{\sigma} + I_{\pi} + \frac{I_{\sigma} - I_{\pi}}{\sqrt{2}} C\left[\cos(2\omega_1 t)\sin(2\gamma) + \cos(2\omega_2 t)\cos(2\gamma)\right] + \ldots \quad (1)$$

where bk refers to the background intensity, C is a constant for a PEM set, ω_1 and ω_2 are the PEM frequencies and γ is the polarization angle with respect to the PEM axis. In typical PEM set ups $\gamma = \gamma 0 + \pi/8$, where γ0 is the orientation of the Faraday electric field with respect to the vertical axis of the machine. As is clear from the above, sigma polarization gives positive amplitude and pi gives negative amplitude for the oscillating components.

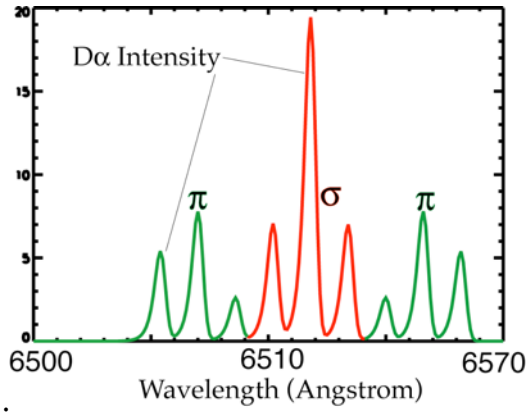

Figure 1 Doppler shifted (arbitrary) D-alpha spectrum

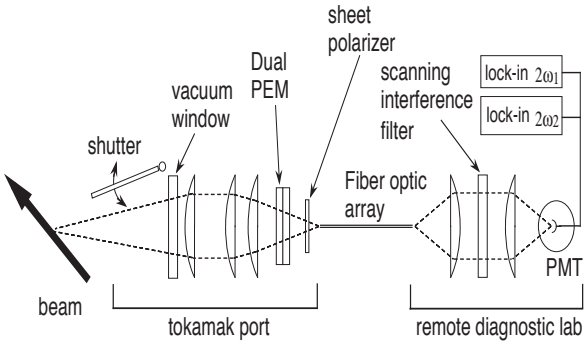

Figure 2 Polarimetric and optical arrangement

The amplified output from the PMT is then frequency analyzed and the aforesaid sine and cosine components are extracted to obtain the polarization angle. The following relations pertain to the MSE measurement:

The polarization angle is calculated from the sine and cosine signals (S1 and S2) using the relation

$$\gamma = \frac{1}{c_1}\left[\frac{1}{2}\tan^{-1}\left(\frac{S_1}{c_2 S_2}\right) - \left(c_3 + c_4 B_\phi^{\,0}\right)\right] \qquad (2)$$

where c1, c2 and c3 are constants that take into account the instrument gains and offsets. The constant c4 accounts for Faraday rotation of the polarization by the viewing window and other optical components with non-zero Verdett constant, corresponding to a nominal toroidal field $B_\phi^{\,0}$.

The plasma magnetic and electric fields are obtained from the polarization angle (pitch angle) from the expression

$$\tan\gamma = \frac{A_1 B_Z + A_5 E_R}{A_2 B_\phi + A_3 B_R + A_4 B_Z + A_6 E_Z + A_7 E_R} \qquad (3)$$

B and E are magnetic and electric fields with subscripts indicating components. A's are coefficients which depend on the beam velocity and beam viewing geometry. A near midplane view ensures that the radial component of the magnetic field is small and since in Tokamaks the toroidal component is very nearly equal to the vacuum field, the MSE measurement is mainly dependent on B_z and E_R. Measurements at the same location using two views with different A coefficients are then used to separate B_z and E_R contributions.

In most tokamaks, an absolute measurement accuracy of better than 0.2 degree and a channel-to-channel accuracy of 0.1 degree are desired. A random error of 0.3 deg is acceptable for most applications.

6.4.2. Calibration of the MSE diagnostic:

In order to carry out actual measurements in plasma, the MSE diagnostic needs to be calibrated. In a basic sense, this can be carried out two ways:

- The diagnostic can be calibrated by placing a polarized light source inside the tokamak vessel. For a given location of the source along the beam line, the polarization angle of the light can be varied and the coefficients c1 and c2 can be determined from the measured values. With a fixture that is rigid so that the reference axis for the light polarization angle remains fixed, the channel-to-channel variation of the offset =c3/c1 can be determined. The absolute offsets would not be known since the direction of the Faraday electric field of the beam is not represented in this measurement. c4 can be measured by fixing the polarization angle and applying different toroidal magnetic fields (see section 3.3)

- Alternatively, polarization (pitch) angle measurements made by injecting the neutral beam into a gas with different values of applied toroidal field and zero poloidal field allows a determination of c3 and c4. Similarly, applied poloidal field can be varied to determine the instrumental gain given by c1 and c2. Since the calibration uses the same diagnostic set up as in actual measurement, the method would, in principle, give an absolute calibration.

Typically, in most tokamaks both of these measurements are carried out. However, it is found that when applied to actual plasma discharges both of these techniques do not give a final calibration and the calibration has to be adjusted in order that the MSE measurement agrees with expected and/or observed MHD and current profile behavior of the plasma.

6.2.3. Beam in Gas calibration of the MSE diagnostic:

The need for adjustment of calibration indicates that there are systematic errors in beam in gas calibration. If source of these errors can be found and corrections are applied or errors eliminated, the beam in gas would be the most suitable for calibrating the MSE diagnostic, particularly when no other calibration method may be available, e.g. in ITER tokamak where there is no easy way of carrying out in-vessel calibration. Also, with Beam in Gas method, the calibration can be carried out between plasma shots.

6.2.3.1 Experience and anomalies with Beam in Gas calibration in DIII-D tokamak.

The DIII-D tokamak has 3 MSE diagnostic arrays from 3 different windows as shown in Figure 3. The 315 and the 45 degree arrays have nearly tangential views. In DIII-D, the constants c1 and c2 are determined using in-vessel calibration and the beam in gas calibration has been used mainly for determining the pitch angle offset (c3+c4* B_ϕ^0). In a typical application, first, the filters are tuned to maximum positive signal

corresponding to sigma polarization. 50 ms wide beam pulses (81 keV, approximately 1 MW) with a repetition rate of 5 to 10 pulses per second are injected into deuterium gas at a pressure of 0.5 mTorr, a desired value of toroidal field is applied and data is acquired. Figure 4 shows example traces of the beam pulse, the toroidal field and the sine quadrature signals for three representative channels from each of the arrays. Two overlaid shots with two flat top values of toroidal fields are shown. (The neutral beam pulses and toroidal field are shown as a function of shot time while the MSE signals are shown as a function of toroidal field). The cosine quadrature signal is similar since the pitch angle is held constant.

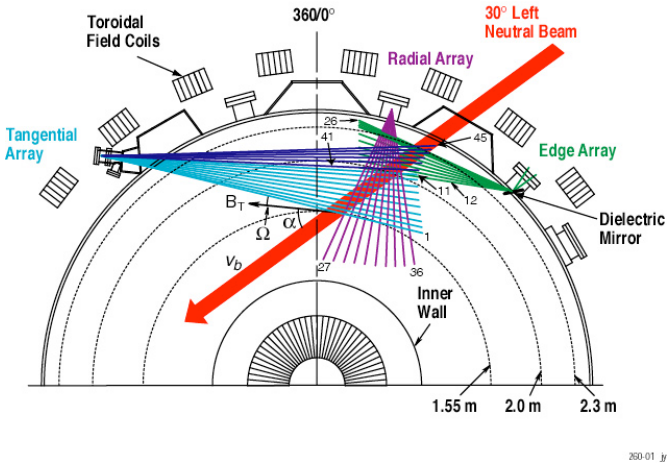

Figure 3. MSE arrays on DIII-D. 315° array is labeled tangential, 45° array is labeled Edge, and 15° array is labeled Radial.

The signals have two important features. At low toroidal fields the signals go negative in some channels, indicating a signal corresponding to a net pi polarization. The second feature is that the variation is not the same for all channels. While the variation is very different between different arrays, there are also significant differences between channels in the same array.

As the toroidal field is decreased, the Stark splitting reduces and with an interference filter of bandwidth comparable to Stark splitting, the intensity is expected to reduce with decreasing toroidal field. If the filter wavelength is offset from the central line, the signal might become negative as the toroidal field is reduced. However, as will be shown, there are other factors.

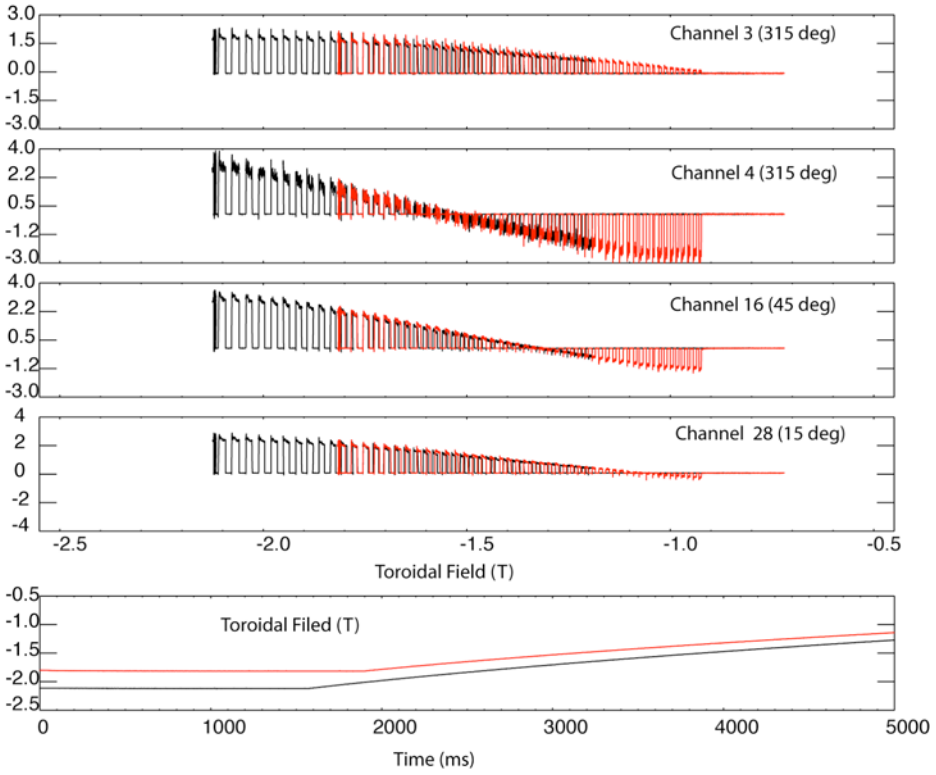

Figure4 MSE signals vs. toroidal field and toroidal field vs. time (shots 102704, 102706)

Figure 5 shows the variation of the measured pitch angle with different flat top toroidal field for the channels shown above. It can be seen that while channel 27's offset and toroidal field are reasonably determined, for other channels there is anomalous dependence of the pitch angle on the toroidal field. It must be noted that this is only true for the beam in gas measurement and for plasmas the variation of pitch angle is found to be consistent with expected Verdet constant of the window. (See section 3.2).

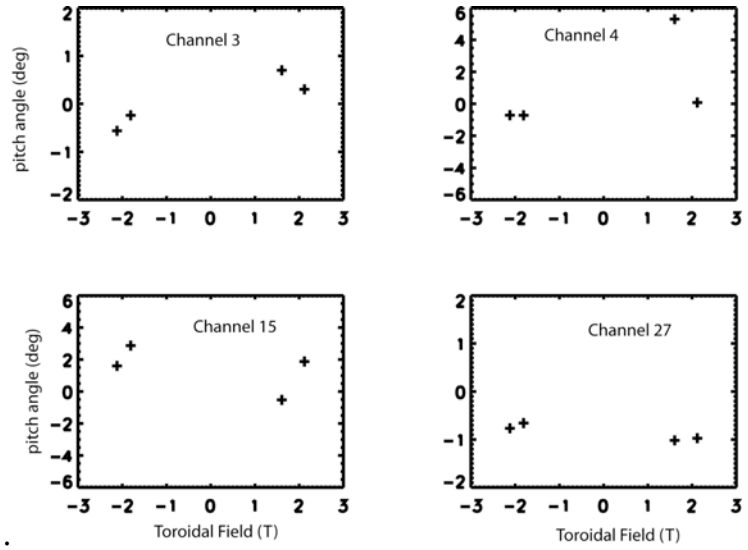

Figure 5 measured pitch angle at different toroidal fields, averaged over flat top durations (shots 102704, 102706, 102780, 102788)

Figures 6 and 7 show the variation of the measured pitch angle as a function of applied toroidal field in the shots shown in Figure 4. From these figures it is evident that again the radial channel (28) gives reasonable measurements and the edge channel (16) has a strong anomalous dependence on the toroidal field. Even though both channels 4 and 16 have sharply decreasing signals with toroidal field, leading to negative signals at low B_ϕ, Channel 4 is less anomalous in the variation of pitch angle with toroidal field.

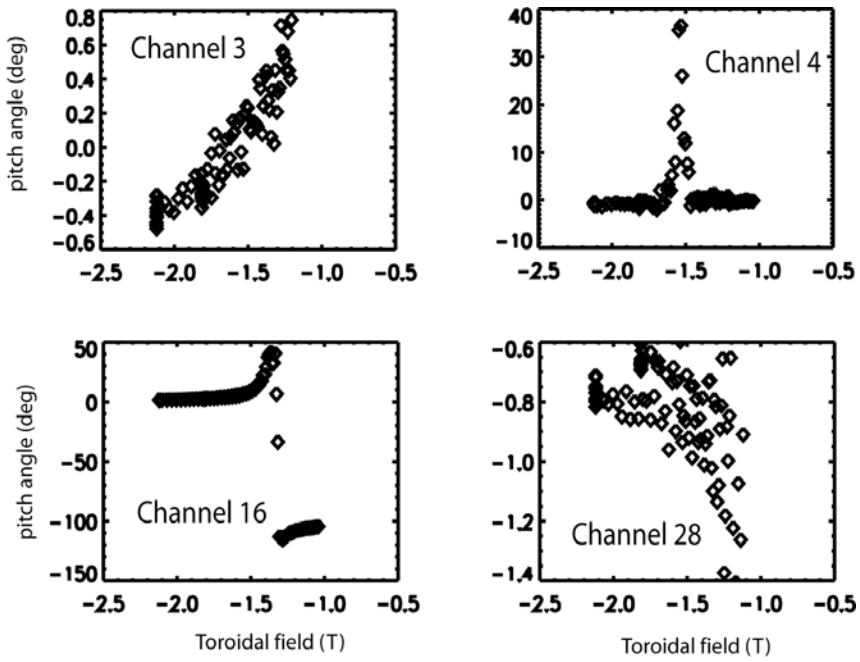

Figure 6 Variation of pitch angle with toroidal field within the shots 102704 and 102706.

Another method to measure the toroidal field dependence (Faraday effect of optics) is to introduce a polarizer at the window (arbitrary fixed polarization angle at zero field) and vary the toroidal field in a beam in gas measurement and this gives reliable results (see Figure 10). The method does not give offsets. On DIII-D this measurement could be carried out only on the 15 deg and 45 degree arrays that have such polarizer elements at the window.

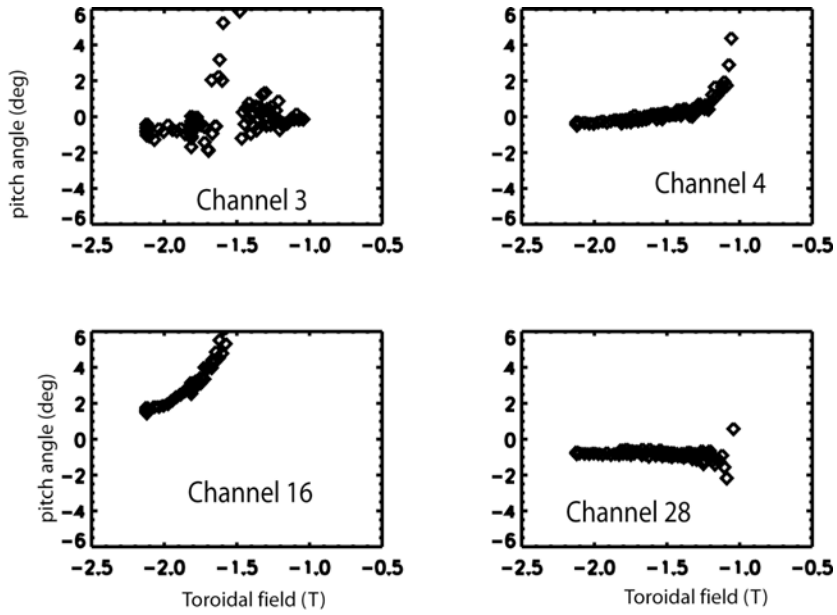

Figure 7. Same as Figure 6 but with a common vertical scale

6.2.3.2 In-vessel calibration of MSE system with toroidal and poloidal fields and comparison with beam in gas measurements:

The strong anomalous pitch angle dependence on toroidal field observed in beam in gas measurements made it necessary to find alternative methods. The usual in-vessel calibrations are carried out with a lamp arrangement that cannot be used in the presence of magnetic field. Also, the arrangement required moving of the source from channel to channel requiring a vessel entry between each magnetic field shot. Therefore, a new apparatus was built to do an in-vessel calibration of pitch angle dependence on the toroidal field (Faraday rotation of the optical elements).

A series of (Moxtek) polarizers, which are not affected by magnetic field, were mounted corresponding to each channel (one array at a time) on rails and mounts that were not affected by slowly ramped magnetic fields. The polarizers were lit by fiber optic light panels (paddle shaped) that also could work in presence of magnetic fields and were illuminated by fiber bundles that were fed into the vessel from outside. The variation of polarization angles was measured while the toroidal and poloidal fields were applied. The following is a summary of results of these measurements

•We were able to confirm the Faraday rotation due to optics.
•For radial array (15 deg-Ch 27-36), the Btscale measurements agree with beam in gas measurements.
•For tangential array (315 deg- Ch 1-11), the present measurements give larger (30-50%) Btscale compared with beam in gas values.
•With this test, reliable Btscale (c4) measurements have been obtained for the edge array (45 deg- Ch 12-26) and these compare well with polarizer-in measurements with beam in gas. The measured Btscales are in good agreement with estimates based on geometry.

Figure 9 shows a typical example of the measurement and comparison with beam in gas results. The beam in gas computation of the coefficient c4 was based only on data at +/- 2.1 T toroidal field, because of increasingly anomalous (non-linear) dependence at low toroidal fields.

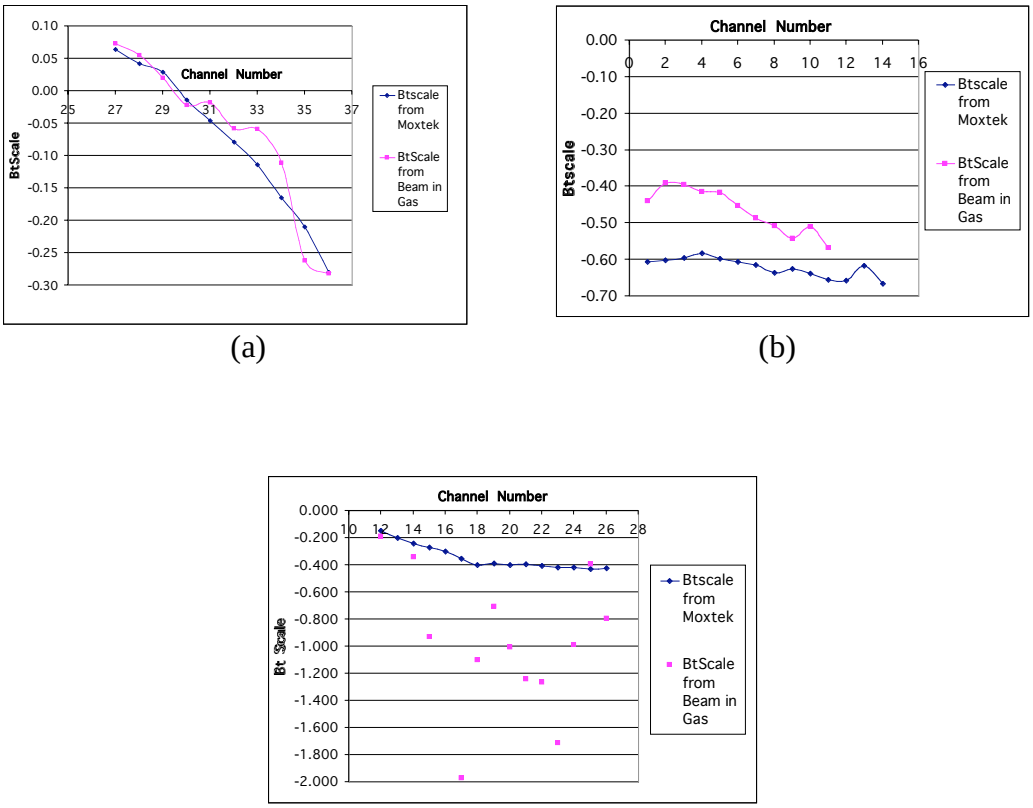

Figure 9. Comparison of in-vessel with field measurements of coefficient c4 (blue) and that obtained by beam in gas measurements. (a) 15 deg array (b) 315 deg array (c) 45 deg array

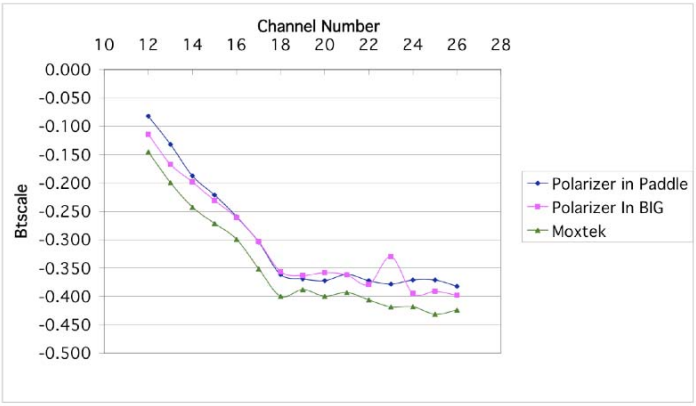

Figure 10 Comparison of Beam in the gas with window polarizer (Magenta), in-vessel polarizer (green) and in-vessel fiber optic paddle source and window polarizer. (45 deg)

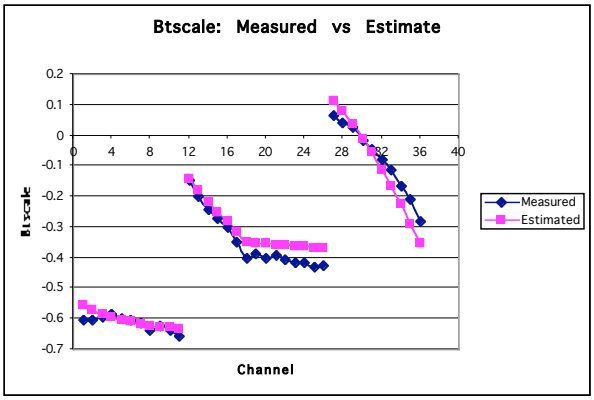

Figure 11 Comparison of measurements of Btscale (c4) coefficients using in-vessel polarizers with estimate of the Faraday rotation at the window using 1 deg/ Tesla Verdet constant.

The figures show that the measured c4 coefficients using Moxtek polarizers are in good agreement with estimates (Figure 11) and window polarizers also give good measurements of the coefficient. With these coefficients reasonably well established, it is clear that beam in gas measurements give reasonable measurements for the radial channels (15 deg), poorer measurements for the tangential (315 deg) array and very poor measurement for the edge (45 deg) array which has a mirror in the optical train.

6.2.3.3 Scatter in beam in gas measurements and comparison with plasma:

In general, the beam in gas MSE signal is 5-10 times smaller than the corresponding highest signal (optimum plasma density) in plasma. This results in a larger photon shot noise, but there is also a scatter (Gaussian noise) in measured polarization angle. Since the signal decreases with decreasing toroidal field, this scatter increases. Figure 12 shows that scatter distribution is different for different channels. Channel 13 also has a strong change in average value with toroidal field, similar to in Figure 6. While

channels with anomalous beam in gas measurements have broader scatter distributions, the width is not an indication of anomaly.

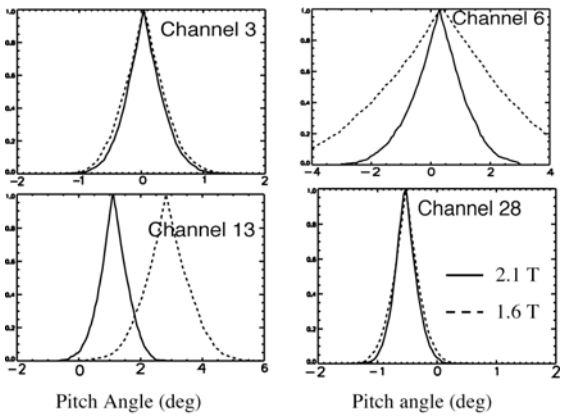

Figure 12. (Gaussian) pitch angle scatter distribution of Beam in Gas measurements

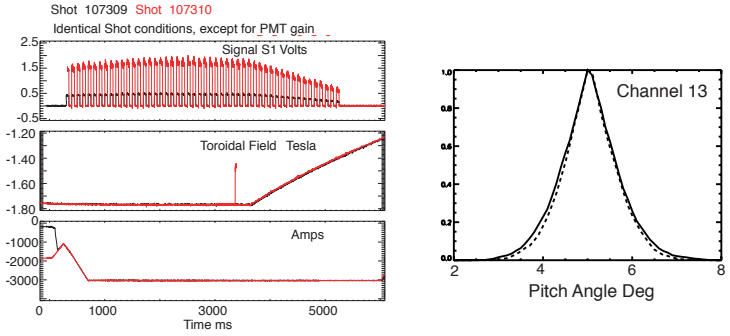

(a) (b)

Figure 13 The scatter distribution is independent of the PMT gain

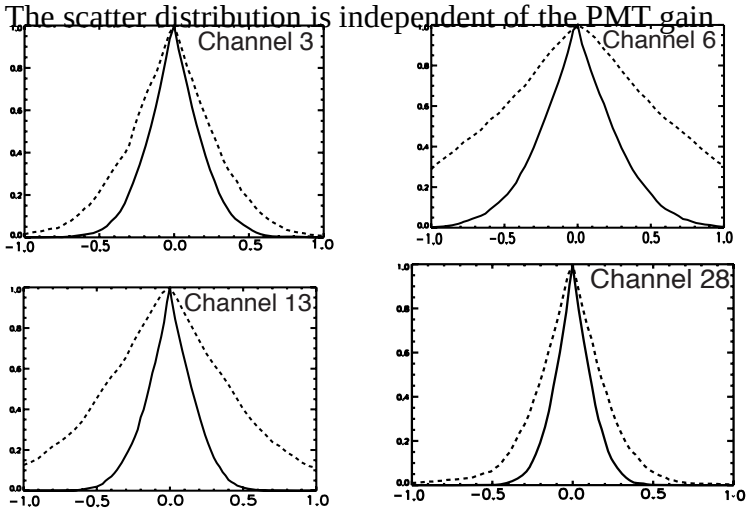

Figure 14. Comparison of pitch angle scatter distribution for beam in gas (dashed) compared to that in plasma (solid). (offsets are adjusted).

.2.4. MSE D-Alpha spectrum:

The MSE spectrum (neutral beam emission) depends on the target such as gas or plasma. While calculation of the light spectrum has been carried out for the plasma in tokamak relevant conditions, there are no calculations for beam in gas. However, the experimental measurements are available [6,7]. Since the important detail is the resolution of the spectrum to the level of polarization rather than individual lines, i.e. the selection of the lines has to capture only the polarization of choice, it is sufficient to look at the polarization as a function of wavelength. Such a polarization "spectrum" is obtained by tilting the interference filter, which decreases the filter wavelength. (There is also a concomitant increase in filter bandwidth). Figure 15 shows the comparison of measurements of the D-Alpha beam spectrum for injection into a gas vs. plasma obtained by this "filterscan".

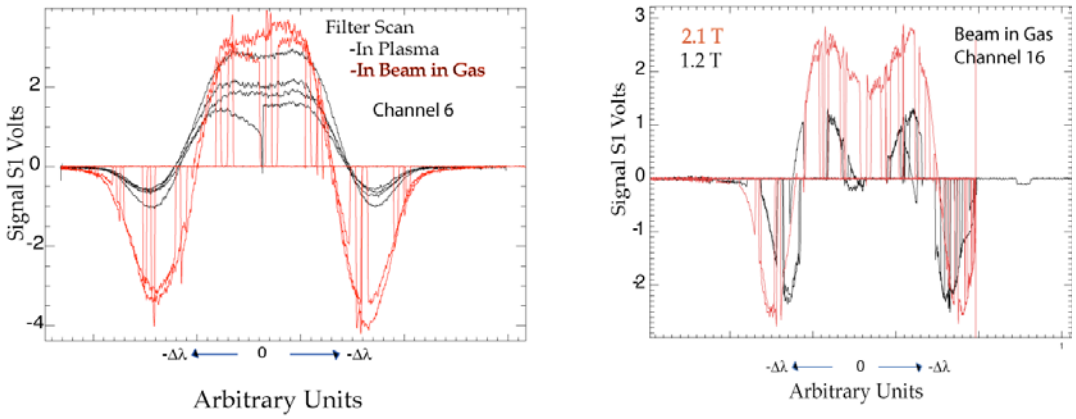

Figure 15. "Filterscans" with beam in gas and plasma (left) and at two toroidal field values (right) for an anomalous channel. Because the tilting of filter only reduces the wavelength these represent scans to shorter wavelengths.

These scans show that the pi polarization intensity (negative signal) relative to sigma polarization is much higher in beam in gas than in plasmas. This has also been observed in other tokamaks (see e.g. Ref.6) This means that for a filter bandwidth comparable or larger than the Stark splitting, the mixing of pi and sigma components at any given wavelength is higher than for plasma. Section 5 describes how this could affect the measurements. The dependence of the scan on the toroidal field in beam in gas for a channel which anomalous results is more difficult to understand. To compare the measurement with expected scans, filterscan was simulated.

6.2.4.1 Simulation of MSE spectrum and calculation of pi/sigma component.

The MSE spectrum was calculated from the Bethe-Salpeter (statistical) distribution of population of Stark levels. The lines were broadened to account for beam temperature and then the light output through an interference filter of given bandwidth was calculated. The pi and sigma intensities were calculated separately and the PEM

signal was simulated by subtracting one from the other. The scan was simulated using this “spectrum” and contribution from half and third energy components of the beam were included. The intensities of pi lines were enhanced by a factor over that of sigma lines to simulate observed spectrum. Figure 16 shows the temperature broadened lines and the net signal after the interference filter for two toroidal fields (deuterium beam energy of 80 keV; temperature broadening of 0.5 Angstrom, filter bandwidth of 3.0 Angstrom and pi line intensities were increased by a factor of 2.0). The pi lines have negative signals corresponding to the MSE filterscan. Figure 17 shows the resulting calculated filterscan for a channel that has a filter with a wavelength 1 Angstrom less than the central wavelength, for two toroidal fields. Figure 17 also shows the measured filterscan of Figure 15. It can be seen that these two compare very well indicating that an assumption of pi lines being 2 times stronger than a statistical distribution is a good model for both the field values. This gives a significant conclusion that (at least) in beam in gas there are no anomalous changes in intensity as a function of wavelength.

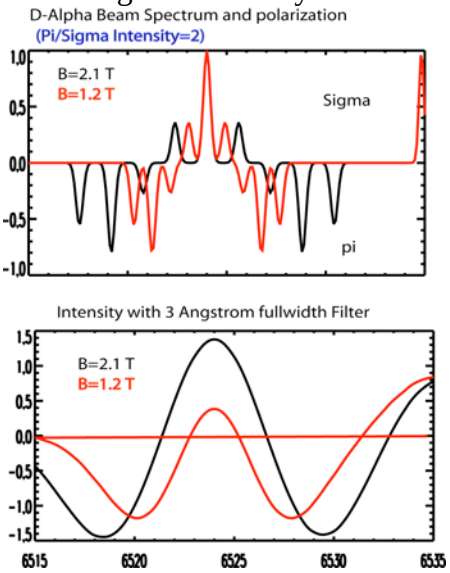

Figure 16. Temperature broadened spectrum (top) and signal calculated after light passes through an interference filter with a bandwidth of 3.0 Angstrom.

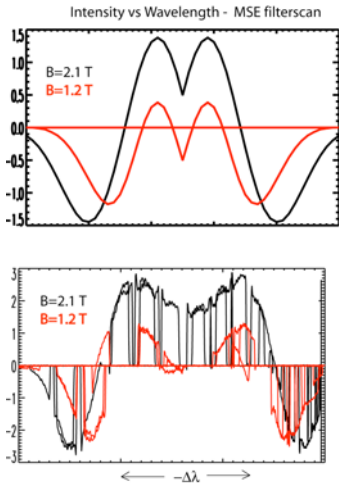

Figure 17. Comparison of simulated (top) and actual MSE filterscans.

The magnitude of the MSE signal then depends on the combination of toroidal field, pi to sigma line ratio, the bandwidth and wavelength of the filter. An illustrative example is shown in Figure 18. It may be noticed that even at the maximum field of 2.1 T in DIII-D, there is a significant component of the pi line. The net negative signal at 1 Tesla corresponds to comparable intensities of sigma and pi lines.

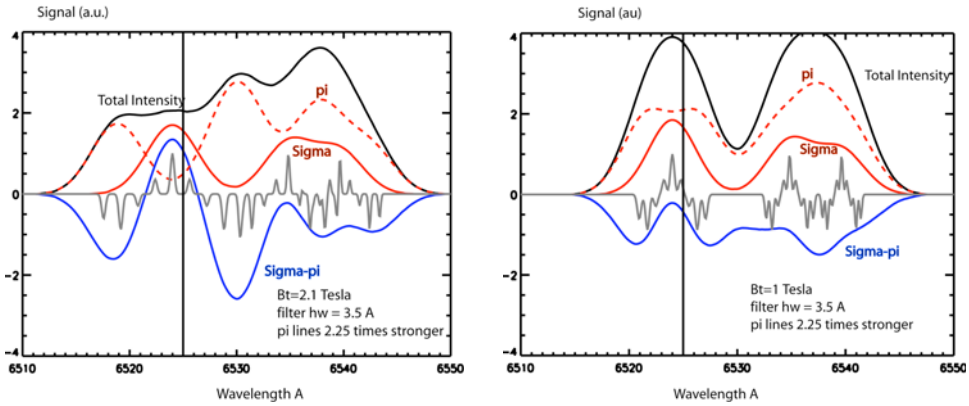

Figure 18 Simulated MSE spectrum, pi and sigma components for a toroidal field of 2.1 T (left) and 1T (right). Filter bandwidth is 3.5 Å and pi lines are enhanced 2.25 times over sigma lines, compared to Bethe Salpeter calculations.

6.2.5. Possible source for anomalous toroidal field dependence of measured pitch angle:

Equation (1) gives the total signal out of the PEM and is actually written as

$$I \sim I_{bk} + I_{\sigma} + I_{\pi} + \frac{I_{\sigma}}{\sqrt{2}} C\left[\cos(2\omega_1 t)\sin(2\gamma) + \cos(2\omega_2 t)\cos(2\gamma)\right] + \frac{I_{\pi}}{\sqrt{2}} C\left[\cos(2\omega_1 t)\sin\left(2(\gamma+\frac{\pi}{2})\right) + \cos(2\omega_2 t)\cos\left(2(\gamma+\frac{\pi}{2})\right)\right] + \ldots \quad (4)$$

which assumes that the optical system treats the sigma and pi polarization in the same way. In the lamp calibration, any variation in measured pitch angle is counted as offset (coefficient c3) and a slope (c1 and c2). In reality, if the system response is not due to just electronic gains (say in the lock-in amplifiers), but is a consequence of optical difference (different optical response functions), then while a pure sigma or pi polarization may be measured by using eq. (2), a superposition would not give a valid measurement as is expected from eq(1). Specifically, if the pi polarization is rotated by an angle δ with respect to sigma polarization, then

$$I \sim I_{bk} + I_\sigma + I_\pi + \frac{I_\sigma}{\sqrt{2}} C\left[\cos(2\omega_1 t)\sin(2\gamma) + \cos(2\omega_2 t)\cos(2\gamma)\right] +$$

$$\frac{I_\pi}{\sqrt{2}} C\left[\cos(2\omega_1 t)\sin\left(2(\gamma+\frac{\pi}{2}+\delta)\right) + \cos(2\omega_2 t)\cos\left(2(\gamma+\frac{\pi}{2}+\delta)\right)\right] + \ldots \quad (5)$$

For small values of δ the error in the measured pitch angle can be written as

$$\gamma_{err} = -\tan^{-1}\left[\frac{I_\pi Sin(2\delta)}{I_\sigma - I_\pi Cos(2\delta)}\right]$$

The consequence of the relative rotation is significant even for small values of δ. A relative rotation of polarization angle of pi to sigma or vice versa is possible, for example, in the presence of mirrors.

The sigma and pi signals were calculated for different toroidal fields and different filter bandwidths, and filter wavelengths, from the spectrum calculations described in section 4. The anomalous dependence of Channel 16 is shown together with a calculation of the expected signal and pitch angle for δ=2.5 deg, for an actual pitch angle of 1 deg. The figure shows that this large change in pitch angle with decreasing toroidal field is explained by a relative rotation of the pi polarization.

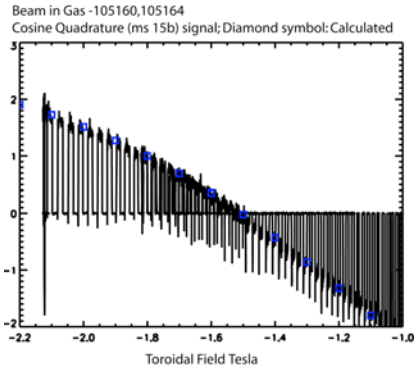

(a)

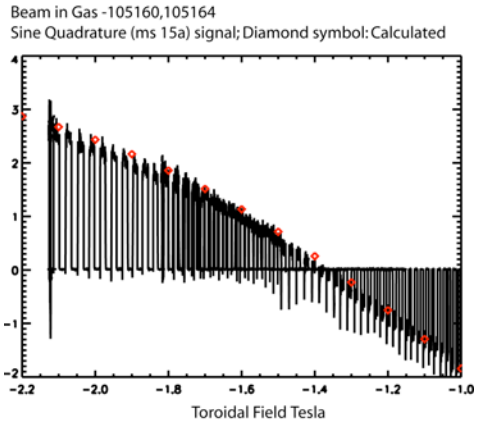

(b)

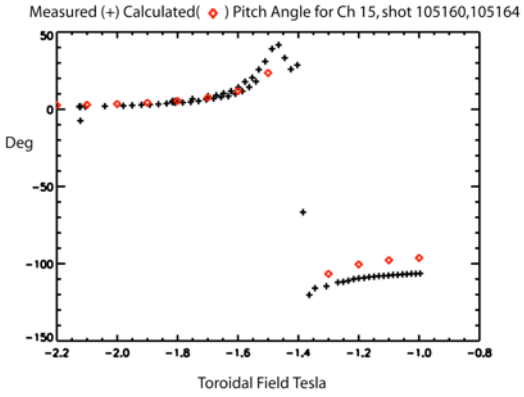

(c)

Figure 19. Measured signals (a) Cosine quadrature (b) Sine quadrature shown in Figure 5 and the calculated signals (diamond symbol). (c) Measured and calculated pitch angles. D=2.5, filter bandwidth=3.5 A, filter wavelength 0.5 deg off the central wavelength.

The deviation (Figure 19c) at large measured pitch angle (low toroidal field) is perhaps due to the effect of c1 and c2 coefficients. Resolution of this will require simultaneous light with zero and 90 deg polarizations during the lamp calibration.

Section 6.3 describes a similar mechanism where the phase of the pi polarization is retarded by an optical element compared to sigma polarization.

6.2.6. Other possible sources of anomaly:

Typically in a tokamak, the D-Alpha light is polluted by other light and much of this is corrected by modulating the beam and thereby correcting for any signal due to plasma light that is constantly present. However, there is no way to correct for additional background or spurious light that is generated when the beam is turned on. Unpolarized light can become partially polarized in an optical train and other polarized light (due to reflection etc) may be present.

6.2.6.1 Linear polarized light noise
The measured pitch angle with spurious linearly polarized light can be written as (for example with only sigma polarization light and noise light with a polarization angle γ_n ,

$$\tan(2\gamma_m) = \frac{I_\sigma Sin(2\gamma) + I_n Sin(2\gamma_n)}{I_\sigma Cos(2\gamma) + I_n Cos(2\gamma_n)} \qquad (7)$$

Reducing this equation gives the result that the measured pitch angle is different from the actual value by the angle (in radians),

$$\gamma_{err} = \tan^{-1}[\frac{I_n Sin(2(\gamma_n - \gamma))}{I_\sigma + I_n Cos(2(\gamma_n - \gamma))}] \qquad (8)$$

As can be seen from above the pitch angle error is highest for a spurious polarization angle which is 45 deg away from the actual pitch angle. This corresponds to approximately a maximum error of 1.5 deg for spurious polarized light intensity which is 5% of the desired D-Alpha light intensity.

6.2.6.2 Elliptically polarized light noise:

While linearly polarized light produces PEM signals at twice the PEM frequency, elliptically polarized light produces PEM signals at the PEM frequencies. So, in general,

elliptically polarized light (e.g. due to a mirror) may not be a problem unless these convert into linear polarized light in the optical train. One other possibility is that the detection system aliases the circular or elliptical polarization signal to twice the frequency thereby creating a false linear polarization signal. This can be checked and calibrated by applying an elliptical light and measuring the response of the detection system and checking the signals at PEM and twice the PEM frequencies.

6.2.6.4 Retardation effect due to other optical components:

If an optical element retards pi polarization by an angle δ_r, the effect similar to the one described in section 5 results.

$$\gamma_m = \frac{1}{2} * \tan^{-1}\left[\frac{(I_\sigma - I_\pi)Sin(2\gamma)Cos(\delta_r)}{(I_\sigma + I_\pi)Sin(\delta_r) + (I_\sigma - I_\pi)Cos(2\gamma)}\right]$$

This change too depends on the filter properties and intensity of pi signals.

6.2.6.3 Light from recombining beam ions:

The beam ions may recombine (e.g. by Charge Exchange) and enter into the viewing volume with a different velocity vector and therefore different polarization angle than for the neutral beam. Work is in progressing identifying this possibility and establishing corrections. [Jinseok Ko, QP1 58, Bulletin of the American Physical Society, Program of the 48th Annual Meeting of the Division of Plasma Physics, 2006.]

6.2.7. Reproducibility of Beam in Gas data and correlation with final calibration used for plasma

6.2.7.1 Accounting for different polarization intensities in beam in gas:

The intensities of pi lines are larger in beam in gas and therefore when making measurements with sigma lines, the effect of leakage of pi lines in plasma will be less and the errors due to leakage of pi lines will be smaller and as a result beam in gas calibration would give inadequate calibration. If pi lines were used for the measurement, the leakage of sigma lines will have less effect in beam in gas but will have a greater effect in plasmas. Therefore the calibration would still be inadequate.

However with a measurement of pitch angle with the use of pi polarization lines and with sigma polarization lines in beam in gas, the effect of mixing of polarization in the optical train can be quantitatively determined, as is approximately done in Section 5. A model (Collisional radiative modeling + filterscan model + PEM model + noise) is near completion in LLNL to make these calculations and will be exercised in DIII-D calibration.

6.2.7.2 Correlation of beam in gas between different calibration periods and with final calibrations:

In most tokamaks, a calibration is obtained as often as feasible. For example, in DIII-D, a calibration is obtained during the vent period (once a year). During the experimental campaign and maintenance of the device, the following changes may take place:

- The tokamak vessel, the toroidal field coils and the beamline may shift changing the geometry of the MSE measurement.
- The interference filters may need to be changed due to changes in their performance.
- There may be drifts in the polarimetric system that may need reoptimization.
- The windows and mirrors may change in their response to polarized light.

From one calibration period to the other, it has been found in DIII-D that several filters need to be changed. Our preliminary retesting of 3 filters indicate that this is most likely not due to changes in the filter characteristics. That, in turn, indicates that there are geometric changes that cause a change in Doppler shift (2% or less). (The beam voltages are controlled to within about 1%- which means that the Doppler shift would change at most by 0.5%). The change in filters may set off a chain of calibration changes since the filters vary in performance. An example would be that the contributions to the background might change with the wavelength or the characteristics of the filter (such as bandwidth) so as to allow more or less unwanted polarization component (pi component in DIII-D). As shown before, such changes may result in calibration changes, even when the polarimteric system remains robust. Such changes are therefore not trackable using an in-line polarizer, which may be used for checking the polarimetric system.

Figure 20 shows the variation of the beam in gas results on the offset (coefficient c3) from year to year. In this comparison, the coefficient c1,c2 and c4 were held the same. (It is reasonable to assume that c4 is constant since this depends mainly on the material properties of polarimetric components). The product of c1 and c2 is nearly 1.0 and are determined with only an accuracy of a few percent. Since the absolute offset is about 22.5 degrees, this amounts to an offset change of around 0.5 degree. The year to year changes can therefore not be determined by a grater accuracy. (However, once determined, to the first order the uncertainty in c1 and c2 and the uncertainty in c3 compensate and are therefore applicable to the measurement). (For the 2006 calibration, channels 3,4 and 5 had instrumental problems and the data should be ignored).

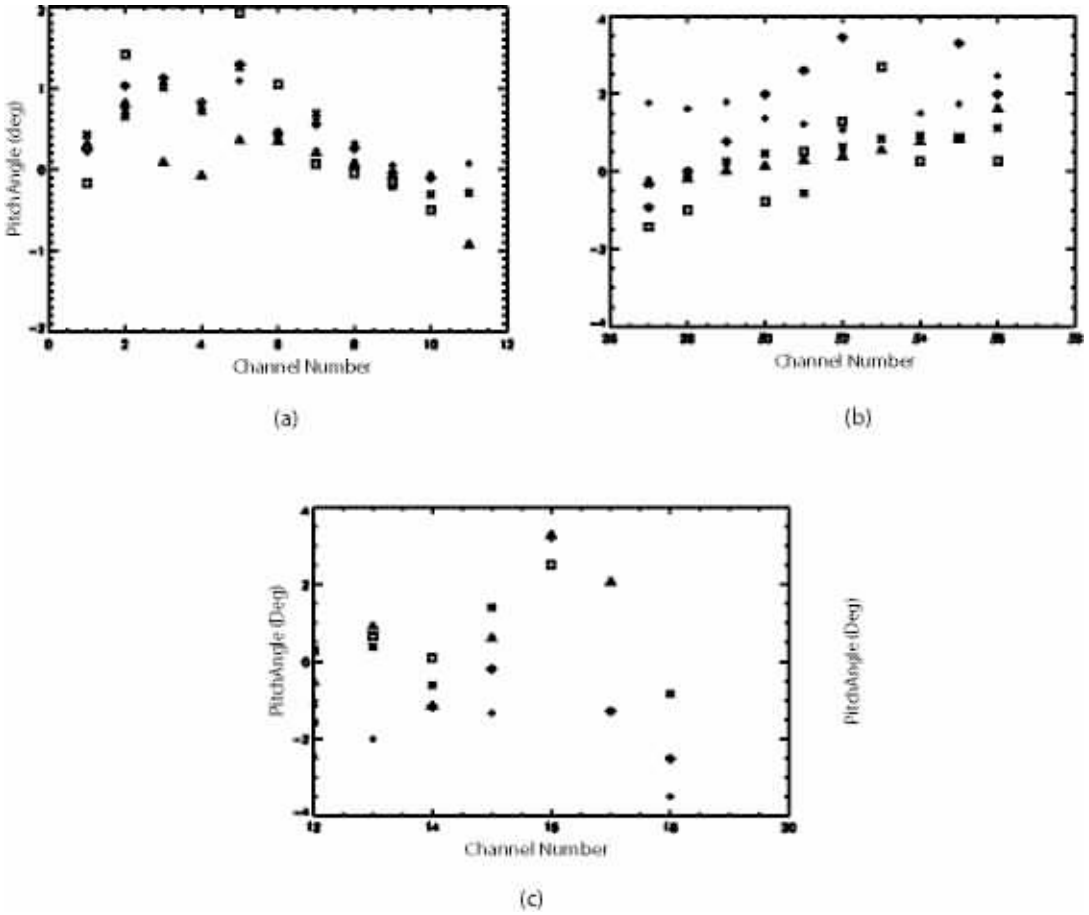

Figure 20- Beam in gas offsets with coefficients c1,c2 and c4 held constant for different calibration periods. Symbol plus- 2000, Asterisk – 2001, diamond- 2002, triangle -2004, square-2006. (a) 315 array (b) 15 deg array (c) 45 degree array

As stated before, after the initial steps, the calibrations are finally adjusted incorporating the "experience" in MSE measurements in plasmas such as correspondence with MHD phenomena and ECE measurements. Such adjustments are global and some of the changes are correlated between different channels and may not necessarily represent the actual required change for each channel. Figure 21 makes a comparison of the correspondence between the beam in gas measurements and the final calibrations for the 3 arrays of DIII-D. It can be seen that while the difference between beam in gas and the final calibration may be as much as 1 degree for the 315 and 15 degree system, the beam in gas agrees with the final calibration well within the calibration need. The large difference for the 2000 calibration in the 15 degree system is due to the fact that in that period there was a small malfunction in one of the PEMs in that array.

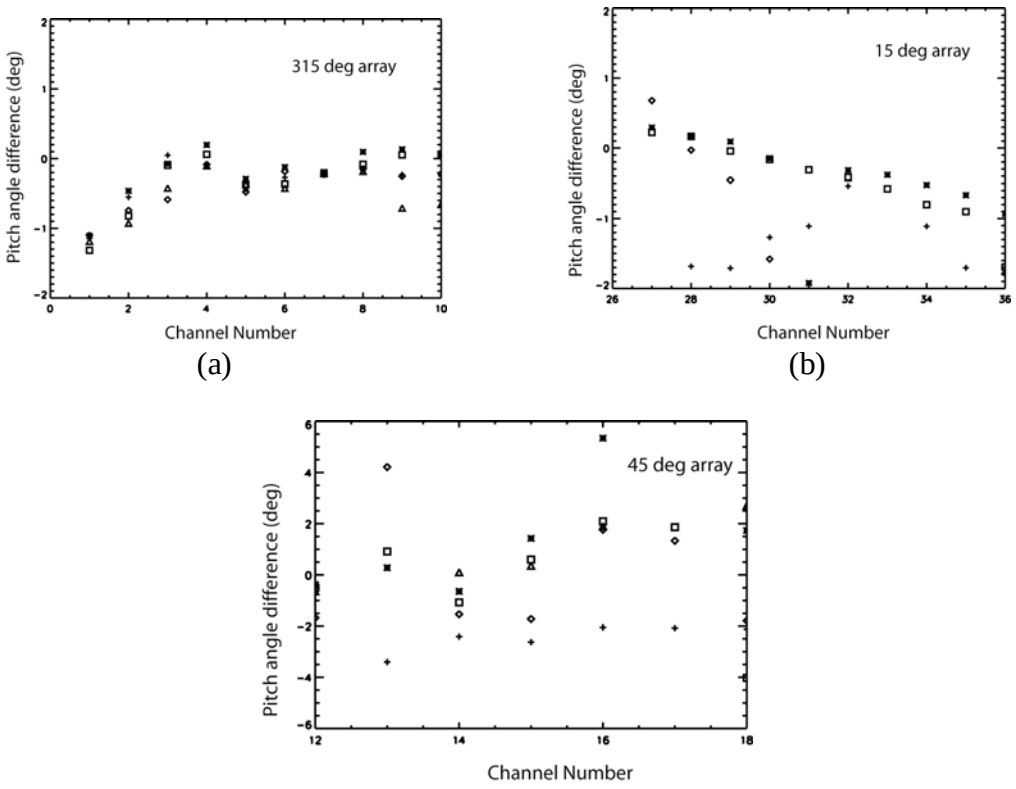

Figure 21- Comparison of Beam in gas offsets with final plasma calibrations. Symbol plus- 2000, Asterisk – 2001, diamond- 2002, triangle -2004, square-2006 (a) 315 array (b) 15 deg array (c) 45 degree array

However, for the 45 deg array, there is much less certainty about the correspondence. Since the final calibration depends on the correspondence of the safety factor with the observed plasma phenomena, and safety factor profile depends on all the channels, it is possible that the effect of the malfunction in the 15 degree system affected the 45 deg array plasma calibration for 2000. Generally, as seen in Figure 20, the year to year difference is also large for this array . The poorer performance of the 45 degree array is caused by a combination of the following features:

- The system has a mirror which probably changes the performance depending upon how much pollution from extraneous polarized light exists.

- The array views the outer plasma so that the toroidal field is lower thereby allowing more mixing of polarization. The coupling of this condition with the presence of the mirror which responds to sigma and pi polarization non-ideally creates significant errors. (section 5).

- The radial electric field is typically larger in the outer plasma and some of the uncertainty is related to errors in obtaining the correct solution from the pitch angle profiles.

- The density is typically lower in this region and in low average density plasmas, this reduces intensities.
- Being closer to the edge, the view is more susceptible to impurity radiation.

Summary:

The present study of beam in gas calibration for the Motional Stark Effect system indicates the following-

- The calibration procedure has the potential to determine the calibration with the required accuracy under certain conditions that are available for the 315 deg and 15 deg array.
- One of the clear reasons for the non-exact correspondence between beam in gas calibrations and the final calibration is due to the presence of extraneous polarization component or components and response of the polarimetric system to these components in unexpected ways.. More rigorous calibration techniques are being developed to discriminate against such components.
- The most likely reason for the difference between beam in gas and plasma calibrations may be due to orbit effects and recombining fast-ions. This is a plausible reason for the radial view (15 degree) which has a poor radial resolution permitting a broader view of different classes of emitting atoms.
- The calibration appears to have better success with tracking the calibration where geometric, beam characteristic, polarimetric and electronic system performance effects can be accounted for.

References:

[1] R. Jayakumar et al., *Current Profile Measurement on the DIII-D Tokamak*, J. Fusion Science and Technology, 2005

[2] F. M. Levinton *et al.*, Phys. Rev. Lett. **63**, 2060 ~1989!.
[3]Wroblewski, D., Lao, L.L., Rev. Sci. Instrum. **63** (1992) 5140.

[4] US-ITER (DoE) announcement

[5]R.L. Boivin, T. Casper, and K.M. Young, *Measurement requirements for the Advanced Tokamak Operation of a Burning Plasma Experiment,* Plasma Phys. Control. Fusion 46 (2004) A347-A353

[6] F.M. Levinton, S.H. Batha and M.C. Zarnstroff, *'Calibration of the upgraded motional Stark effect diagnostic on TFTR'*, Rev. Sci. Instrum. 68 (1), January 1997

[7] R. Jayakumar et.al, *'Analysis of Calibration results and Performance of DIII-D MSE system*', High Temperature Plasma Diagnostics Conference 2002, Madison, WI

6.3 Calibration using a rotating elliptical polarization source: Mueller matrix approach

This section describes a more general approach to calibrating an MSE diagnostic than is typically used that may prove useful for ITER. We are in the early stages of work to try to apply these techniques to the DIII-D MSE diagnostics, so as of this writing only a general outline of the approach is available.

Traditional MSE calibration is usually limited to determining coefficients in a function of the PEM second harmonic signals with a known input linear polarization state. This has proven reliable for simple MSE systems that use zero or one plane dielectric mirror, because these systems do not greatly perturb the input polarization state. A single, plane dielectric mirror may rotate the azimuth and increase the ellipticity of a purely linear input state somewhat, but the resulting azimuth is never too far off (consider Figure 3 in the mirror measurements section, for example). In contrast, consider a multiple mirror MSE system for ITER that uses metal and possibly dielectric mirrors that will likely be curved. The total perturbation to the input polarization state is likely to be much higher than in our present simple systems, possibly requiring a more complex calibration function. With this in mind, it would be ideal to know the complete Mueller matrix M_{MSE} describing each MSE channel.

The use of a dual PEM system requires at most four measurements (I_{DC}, $I_{\omega 1}$, $I_{2\omega 1}$, $I_{2\omega 2}$) to determine the Stokes vector $S_{out} = (I,Q,U,V)$ transmitted by the optical system. Assuming M_{MSE} is invertible, the unknown input polarization state could be calculated by $S_{in} = M^{-1}_{MSE} S_{out}$.

Having M_{MSE} would allow several crosschecks. First, M_{MSE} should be the product of the Mueller matrices of the individual optical elements. These may be known from either models or actual measurements made during the design and fabrication of each component. The second crosscheck would be to reconcile any traditional fitting function for the linear polarization azimuth with the Mueller matrix. As long as the same data acquisition system is used to measure both, in principle the measured traditional calibration should be derivable from the measured Mueller matrix. (Note that gains and offsets due to electronics may be built into the measured Mueller matrix, so it would not be a pure representation of the optical transfer matrix, unless care were taken to separate these effects).

Calculation of the unknown polarization state S_{in} would also return the ellipticity, which is a quantity not normally determined now. This might be useful for determining relative weighting when using these measurements in equilibrium reconstructions (i.e. measurements with a large ellipticity would not be trusted). A large circular polarization fraction coming from the tokamak might indicate reflected light is polluting the signal, or that the atomic processes generating the beam emission are not as expected.

Data has recently been collected on the DIII-D MSE systems that will be used to calculate M_{MSE}. A time dependent polarization generator was built and placed inside the vessel where each channel images the neutral beam (Figures 1 and 2).

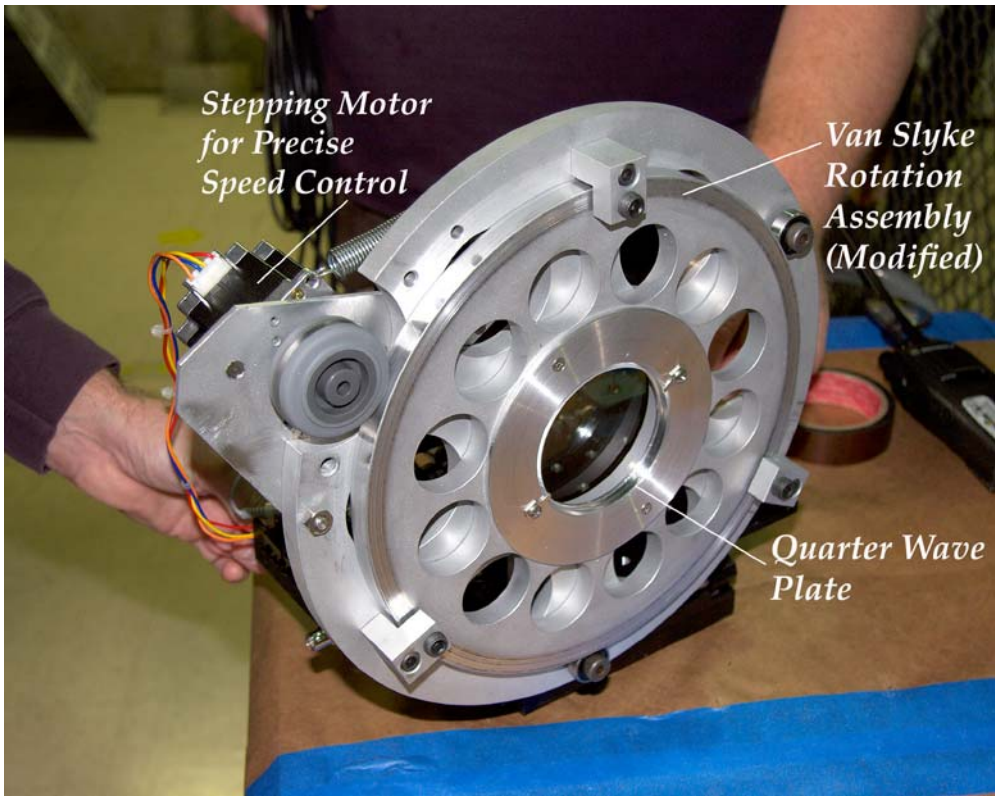

Figure 4.

Figure 5.

6.4 Between and during shot calibration assessment

The generator consists of an unpolarized light source, followed by a stationary horizontal linear polarizer. This is followed by a quarter-wave plate mounted on a set of bearings that is rotated using a precision stepper motor. Our rotation rate was about 2π radians per second, and the total output intensity was recorded for several tens of seconds with a high sampling rate for good statistics. Fourier analysis of the output intensity is used instead of lock-in digitizers to acquire the various frequency components and thus $(I,Q,U,V)_{out}$.

This injects the following time dependent Stokes vector into each MSE channel:

$$S_{in}(t) = \begin{pmatrix} 1 & 0 & 0 & 0 \\ 0 & \cos^2 2\omega t & \sin 2\omega t \cos 2\omega t & -\sin 2\omega t \\ 0 & \sin 2\omega t \cos 2\omega t & \sin^2 2\omega t & \cos 2\omega t \\ 0 & \sin 2\omega t & -\cos 2\omega t & 0 \end{pmatrix} \frac{1}{2} \begin{pmatrix} 1 & 1 & 0 & 0 \\ 1 & 1 & 0 & 0 \\ 0 & 0 & 0 & 0 \\ 0 & 0 & 0 & 0 \end{pmatrix} \begin{pmatrix} 1 \\ 0 \\ 0 \\ 0 \end{pmatrix}$$

$$= \begin{pmatrix} 1/2 \\ 0 \\ \frac{1}{2}\sin 2\omega t \\ -\frac{1}{2}\cos 2\omega t \end{pmatrix}$$

The sectional pattern of the resulting polarization (looking into the beam) is shown in Figure 3.

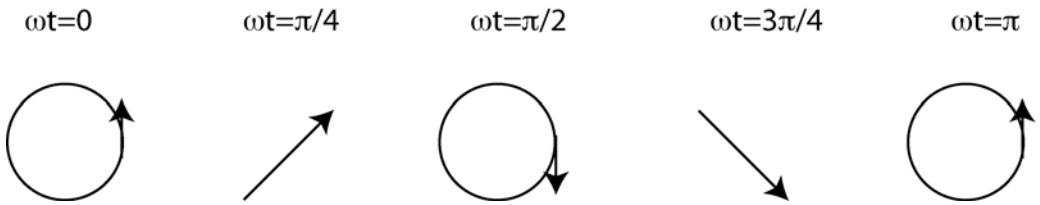

Figure 6.

Determining the Mueller matrix from known input and output states is an oVerdettermined problem. Injecting a wide range of known input states makes a data set that may be sufficiently diverse to allow successful fitting of Mueller matrix models.

A particular challenge for MSE on ITER will be dealing with a possible calibration drift on a time scale measured in number of shots rather than years. This is due to the still uncertain effects of erosion and deposition on the plasma-facing components. Other concerns include neutron damage and component fatigue due to thermal cycling, especially in the case of relatively large curved mirrors. Techniques that would allow an assessment of the calibration either between shots or ideally during a shot are desired.

In present MSE systems on DIII-D, linear polarizers made of Corning's Polarcor glass are built into shutters that may be moved into place during a shot. These face the plasma directly and use it as a source of light. This allows a measurement of a fixed angle on each channel that can be monitored for drifts, and also allows a crosscheck of the Faraday rotation present in the vacuum window. Polarcor has a very high contrast ratio, is very thin (0.2 to 0.5 mm), and the polarizing layers are at the surfaces, rather than inside

the material. This makes it ideal for withstanding thermal cycling and for not being susceptible to Faraday rotation itself. However, according to Corning [http://www.corning.com/specialtymaterials/materials-products/products_overview/polarization/polarcor-glass-polarizers.aspx], laser damage threshold tests indicate that the silver halide crystals in the material melt above 450°C, reducing the contrast ratio. So Polarcor can probably not be used is a situation where it directly faces the ITER plasma.

One approach is to build a retractable shutter that may be inserted either between or during shots with shielding on the plasma facing side. This shutter would normally be housed somewhere in the port plug, and would slide in front of the first mirror in the vicinity of the system aperture stop. On the backside of the shutter and facing the first mirror, either a polarization generator or detector would be mounted. The former would be an LED followed by Polarcor, and the latter would be a photodetector preceded by Polarcor. It is speculated that at least one of these could be found that would survive insertion in front of the first mirror between shots, and possibly during a shot.

In the case of a polarization generator, constant linear polarization would be collected by each channel and analyzed in the usual manner. In the case of a detector, a single fiber optic on each channel would be dedicated to transmitting light backwards through the optics. It would be polarized by the polarizer at the normally downstream side of the PEMs, have its polarization modulated, and be converted to an AM signal by the Polarcor/detector in front of the mirror. This signal would require an additional data acquisition channel to collect it and calculate the reference polarization angle.

If a robust enough emitter or detector were available, it might be possible to dispense with the retractable shutter and mount these permanently on a shielded protrusion jutting into the field of view in front of the first mirror, but still behind the wall. (This would entail a small loss in the number of photons collected from the beam). This would provide a reference monitor while collecting data during a shot. The detector signal could be on continuously, but the emitter signal would have to be timed to be between neutral beam pulses.

A drawback to both of these approaches is that unless the detector/emitter is about the same area as the aperture stop, most of the reference signal will only represent a small fraction of the total mirror surface anywhere in the system. Arrays of small detectors/emitters may be needed to approximate a single large one.

Possibly the simplest idea is to build a shutter that has a polished metal mirror surface on the protected backside. When inserted, a polarized light source located somewhere farther back in the drawer would be directed onto the “reference mirror” and into the optical labyrinth. This approach may match the solid angle of the system better, and it keeps the light source farther away from the plasma. However, it would also require additional open space instead of shielding for the reference light to travel through.

Summary of calibration techniques

Past experience indicates that obtaining and maintaining an adequate calibration for the ITER MSE diagnostic will require an array of complimentary techniques. We have described those already in use, and suggested a few new ones in this section. Given the harsh environment the optics will be in on ITER, it will be essential to use techniques such as those described in 6.1 and 6.3 to calibrate the complete system “on the bench” before installation. There should be an effort to provide remote insertion of these polarization sources into the vessel and in front of the first mirror during down periods to assess changes to the calibration. Beam into gas discharges are the easiest way to routinely check the calibration. With increased understanding of the beam into gas spectrum and the basic polarization properties of the system, beam into gas may eventually be used to absolutely determine the calibration. Even if this level is not reached, beam into gas still offers an easy and routine fiducial to assess relative changes in the calibration due to coatings, erosion, etc. Finally, building a reference into the diagnostic that could be used between or during shots would be very valuable.

Appendix A: Original Statement of Work

SOW# 533-20060630-JOHNSON-1
June 30, 2006, Revision 0

US CONTRIBUTIONS TO ITER PROJECT

STATEMENT OF WORK

FOR

Evaluation of ITER MSE Viewing Optics

June 30, 2006

Prepared by: Stanford (Skip) Schoen
Digitally signed by Stanford (Skip) Schoen
DN: CN = Stanford (Skip) Schoen, C = US, O = Princeton Plasma Physics Lab, OU = US ITER Project Office
Reason: I have reviewed this document
Date: 2006.07.11 07:26:01 -04'00'

S. E. Schoen
PPPL Planning & Control Officer, US Contributions to ITER Project

Approved by: David W. Johnson
Digitally signed by David W. Johnson
DN: cn=David W. Johnson, c=US, o=Princeton Plasma Physics Lab, ou=ITER Contributions Department, email=djohnson@pppl.gov
Reason: I am approving this document
Date: 2006.07.15 20:54:30 -04'00'

D. W. Johnson
Diagnostics Team Leader, US Contributions to ITER Project

1. GENERAL INFORMATION

1.1 Introduction

The United States has joined the International Thermonuclear Reactor (ITER) collaboration as a Presidential initiative. The US activities are managed through the Department of Energy (DOE) Office of Fusion Energy Sciences (OFES). The DOE has selected Oak Ridge National Laboratory (ORNL), managed by UT-Battelle, LLC, to host the US ITER Project Office (USIPO) and be responsible for all aspects of US ITER contributions, acting as the US domestic agency, and leading the US Contributions to ITER Project (the Project). Among the in-kind contributions to be provided by the Project are diagnostic components for measuring various plasma parameters needed to control and understand the reacting plasmas. The Princeton Plasma Physics Laboratory (PPPL) is a partnering institution in the Project, responsible for providing 16% of the in-kind diagnostic hardware for ITER.

1.2 Scope

One of the diagnostic systems being provided by the US is the Motional Stark Effect (MSE) Polarimeter which measures the magnetic field pitch angle profile parameterized by the safety factor q(R). The purpose of this study is to evaluate and optimize the optical design for the front-end viewing mirror labyrinths, the highest risk part of the MSE diagnostic.

The MSE mirror optics are particularly at risk because of the effect of erosion and deposition on the surfaces of the mirrors. Deposited films can seriously impact the polarization properties of the light being imaged and relayed through the labyrinth. The impacts are dependent on the angle of incidence, the coating composition and thickness, and other factors. The present design utilizes six mirrors in an effort to provide an effective labyrinth while minimizing the angles of incidence for the mirrors. Reduced angles of incidence reduce polarization mixing for metal mirrors and also reduce the effects due to coating.

Figure 1 shows the geometry in the reference design for the two MSE views of ITER neutral heating beams and also the geometrically-determined spatial resolution for these views. The details of this geometry along with the optical design parameters for the optical labyrinths for the edge and core views are in reference 1.3.2 below. A plan view of the edge-viewing labyrinth is shown in Figure 2.

Using optical design parameters for the reference design available from the Team Leader, an optical model should be constructed including polarization analysis. Using relevant spatial constraints also provided by the Team Leader, alternate relay models would be explored and compared with the reference in terms of the optical throughput and the polarization mixing.

The far-forward location of the first two mirrors in each of the MSE labyrinths almost certainly constrains these to be metal mirrors, perhaps with a special metal coating (rhodium coating on metal substrate would have high reflectivity and low erosion rate). To dissipate the heat due to surface heating from plasma radiation and volume nuclear heating, these mirrors would have to

be in close contact with actively cooled surfaces or actively cooled themselves. Gold, aluminum and even dielectric mirrors may be feasible as secondary mirrors in these relay systems. (See ref. 1.3.5 for initial studies of dielectric mirrors in RF)

As a free parameter in the search for alternate optical designs, the radial location of the vacuum window can be adjusted from its reference position at the rear of the plug to a more forward position. This would explore the use of retractable refractive optics in a re-entrant tube as part of the relay train.

To understand mirror labyrinth effects on polarization, considerable modeling is needed. The issues are sufficiently complex such that confirmatory experiments are also needed, as has been started by Kuldkepp, et al. (ref. 1.3.6).

Development of a credible, in-situ calibration concept for the MSE system has not yet been done. An effective calibration system would provide information sufficient to compensate, during data analysis, for complex reflectivity changes due to coatings. The time-scale for the creation of these films is difficult to predict. However, based on experiments on existing devices, films that could cause significant polarization impacts could evolve during a small number of ITER discharges. Using what is learned from the optical design and the modeling/experiment on the mirror-labyrinth effects on polarization, a proposal for an in-situ calibration procedure should be developed.

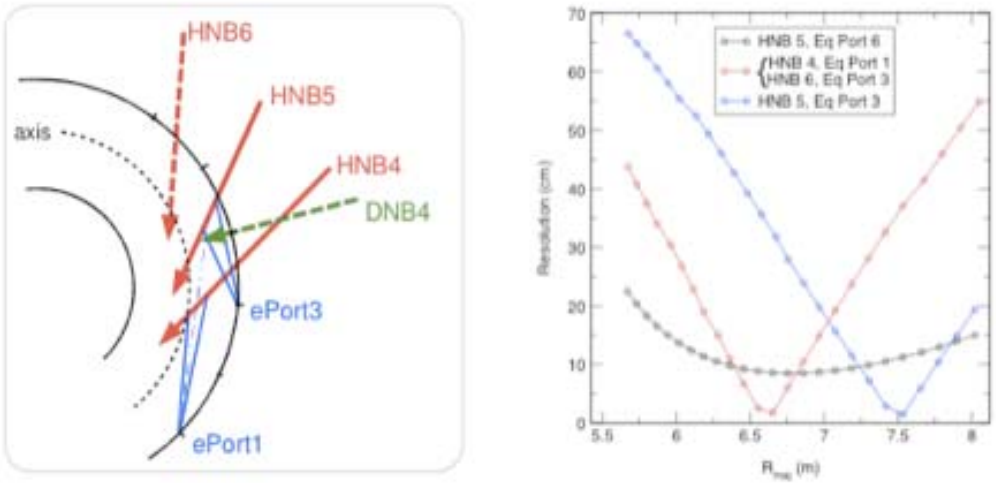

Figure 1 Geometry and spatial resolution for MSE views in reference design

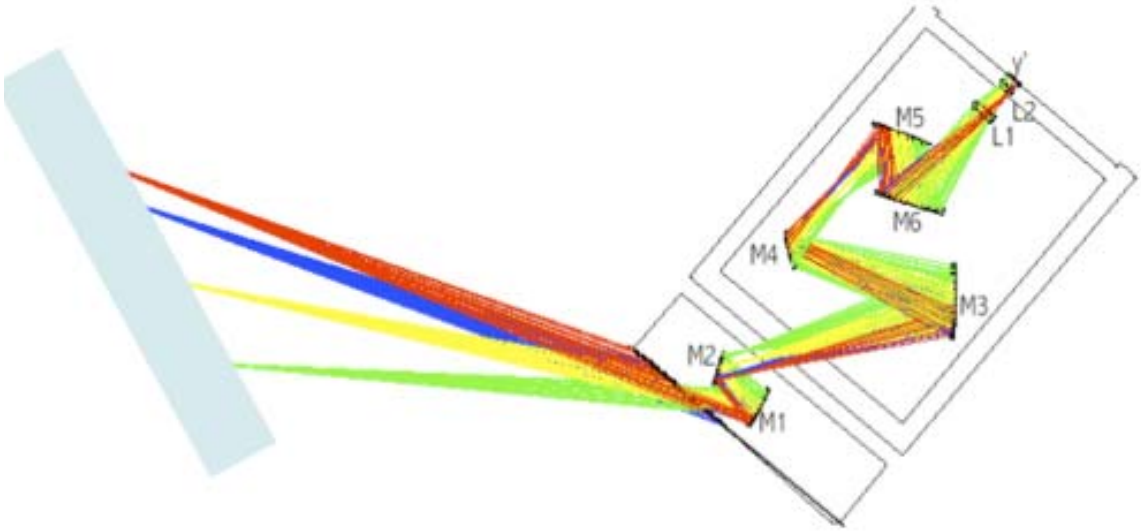

Figure 2 - Plan view of edge MSE optical labyrinth in plug E3

1.3 Applicable Documents and Data

1.3.1 *ITER-FEAT* Diagnostic Procurement Package 5.5.PE IDoMS N 55 SP 3 00-07-19 W 0.1

1.3.2 Final Report, Contract FU05-CT2003-00025 (EFDA/03-1028), Artur Malaquias

1.3.3 A. Malaquias, et al., RSI, 75, 3393 (2004).

1.3.4 Design Analysis of the ITER Motional Stark Effect diagnostic, Final Report, Contract EFDA 02-1005, N. C. Hawkes, March 3, 2004

1.3.5 I. Orlovskiy and K. Vukalov, ITPA10 Moscow Diagnotics Meeting, RF Progress Report.

1.3.6 M. Kuldkepp, et al., RSI, 75, 3446 (2004).

Note: The above reports and other relevant material can be found at:
http://www.pppl.gov/usiter-diagnostics/Instrumentation-Packages/

2. REQUIREMENTS AND RESPONSIBILITIES

The Oak Ridge National Laboratory has been selected by DOE-OFES to support the Federal Project Director (FPD) in managing all day-to-day aspects of the project. The US ITER Project Office (USIPO) will be managed by ORNL; the Contractor Project Manager and key support staff will be co-located with the FPD at ORNL. UT-Battelle, LLC, as the operating contractors for ORNL, has oversight responsibility for ensuring that the project meets all technical, cost, and schedule objectives. Major procurements will be approved by the ITER central team and otherwise managed by the US ITER Project Procurement Director at ORNL. The Diagnostics Team Leader is located at Princeton Plasma Physics Laboratory (PPPL) and, along with the PPPL procurement office, has management responsibility for diagnostic procurements.

Financial and Performance Reporting. Monthly reports shall be compiled and submitted to PPPL by the subcontractor. PPPL will issue project performance data to the USIPO at ORNL, which reports to the DOE FPD, who will issue monthly project performance reports to the OFES Program Manager. These reports shall include financial information utilizing earned value methods, as well as documentation of technical progress, required deliverables and milestones. Anticipated or actual cost and/or schedule variances that would be in excess of thresholds should be clearly identified as soon as known, and reported to the PPPL.

3. WORK DESCRIPTION

Listed below are the specific work tasks to be performed under this statement of work

3.1. Using optical design parameters available from the Team Leader, create an optical model including polarization analysis.
3.2. Using relevant spatial constraints also provided by the Team Leader, explore alternate relay models and compare to the reference model with regard to the optical throughput and the polarization mixing.
3.3. Model the transformation of the polarization state of an appropriate plane mirror labyrinth and conduct laboratory polarimetry experiments to test this model.
3.4. Develop a concept for an in-situ calibration scheme capable of characterizing the effects of the mirror labyrinth on the polarization state of the light collected from each of the radial positions where MSE measurements are sampled.
3.5. Write report describing the methodology used in 3.1-3.4 and summarizing the results of these studies, including illustration of high leverage issues.
3.6. Present summary of findings and provide electronic copy of presentation at USIPO/BPO workshops and/or ITPA Diagnostic TG meetings.

4. FUNDING AUTHORIZATION

Funding is distributed to participating organizations based on an approved funding profile. The US ITER Project Office prepares the necessary documents to authorize participating laboratories to cost and commit funds. Official funding authorization is to be provided to each laboratory via DOE Interoffice Work Order (IWO B&R 8201) organization contracts.

For US ITER diagnostic work, the DOE- Princeton Planning and Budget Division is responsible for transmitting the IWO documents to the appropriate DOE field offices. The DOE field offices will accept the procurement request and authorize participating laboratories to perform work consistent with the statement of work and funding limitations. Each laboratory participant will be subject to home laboratory internal work authorization rules (e.g., purchase orders, subcontracts, work orders, etc.). Cost and commitments will be limited by the amount of funds allocated to each participant. The USIPO routinely incrementally funds participating laboratories. Work scope is generally funded at less than full funding in the first half of the fiscal year. Costs, commitments, and progress are reviewed at mid-year and annual funding distributions may be revised accordingly.

5. DELIVERABLES

5.1. Report describing the methodology used in tasks 3.1-3.4 and summarizing the results of these studies, including illustration of high-leverage issues.
5.2. Present summary of findings and provide electronic copy of presentation at USIPO/BPO workshops and/or ITPA Diagnostic TG meetings.
5.3. Monthly reports as detailed in Sect. 2-Requirements and Responsibilities: Financial and Performance Reporting.

Formats for deliverables:

- Electronic file sent as an e-mail attachment (MS Word or Powerpoint, or pdf)
- No paper copy is required

Report Deliverables to PPPL	**Due Date**
Monthly reports	Last week of each month starting 2nd month of period of performance.
Final report	10 days before period of performance end date.

Appendix B: Neutronics Analysis (not funded by SOW)

During the design study, it became apparent that one figure of merit of the optical design would be the neutron shielding provided by the bends in the labyrinth. The USIPO has indicated that the actual constraint will be the shielding of the whole port plug, but it would be useful to understand how many “doglegs” are needed in the optical design.

A neutron shielding estimate is a Monte Carlo code calculation that requires the generation of a grid. Currently, these grids are constructed “by hand”, and are quite time consuming. It is extremely desireable to be able to go directly from the CATIA or ProEngineer CAD model to a Monte Carlo calcuational grid, and then be able to use this grid with a benchmarked neutronics code like MCNP or TART. The USIPO plans on using the ATTILLA code to do this work, and expects to have this capability in the summer of 2007. LLNL, supported both by the National Ignition Facility and internal LLNL funding, has explored a tool called TOPACT to do the generation of the calculational grid. Cases have been run for both the NIF target chamber and the original ITER (EU) MSE design.

We are currently working on a design study (not funded by this SOW) to compare the neutron shielding of the EU and LLNL-4(edge) optical designs. The CAD layout of these two designs are shown in Fig. B-1. Currently, both CAD models have been used to created grids with the TOPACT code, and we are running both TART and MCNP for these two cases. It has been our experience so far that minor interferences in the CAD models is usually the source of difficulty for the grid generation software. In addition, the inclusion of detailed, complicated shapes which are not important for the neutronics calculations can also result in problems.

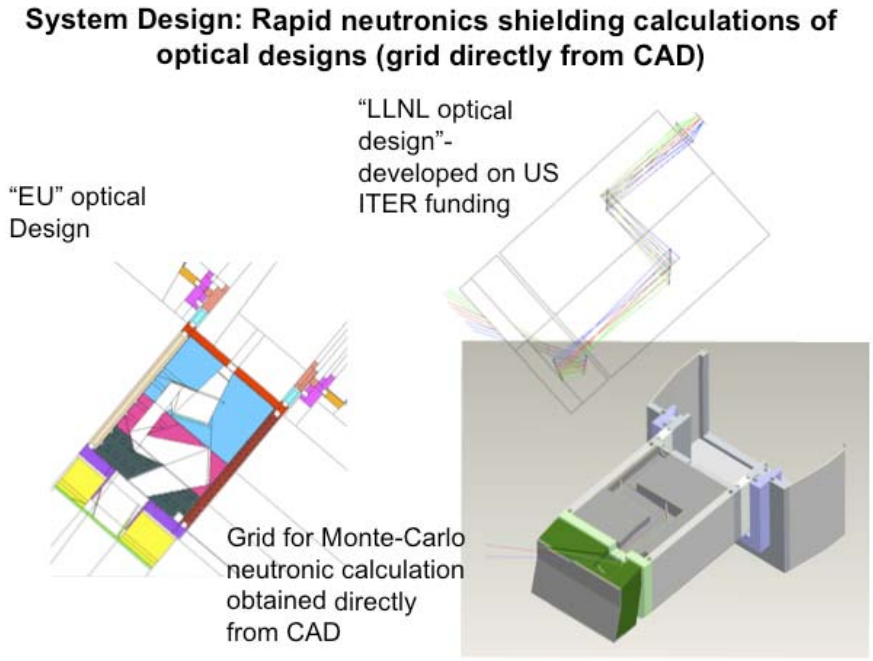

Figure B-1. Neutronics comparison of the EU and LLNL-4(edge optical designs)

Appendix C: Synthetic MSE diagnostic in the CORSICA plasma model (not funded by SOW)

In assessing the measurement requirements of the MSE for ITER, it is important to consider the details of the current profiles expected for the various scenarios. We have developed (on LLNL internal funding) a synthetic diagnostic that calculates the MSE pitch angle from the plasma current profile. The plasma model is CORSICA, and can follow the development of the current profile with either ohm's law or other forms of anomalous resistivity. An example discharge is shown in Fig. C-1, where the pitch angle at several locations as a function of time is calculated. If necessary, we could extend this calculation to a MSE photon brightness by including the atomic physics processes responsible for the Stark Spectrum.

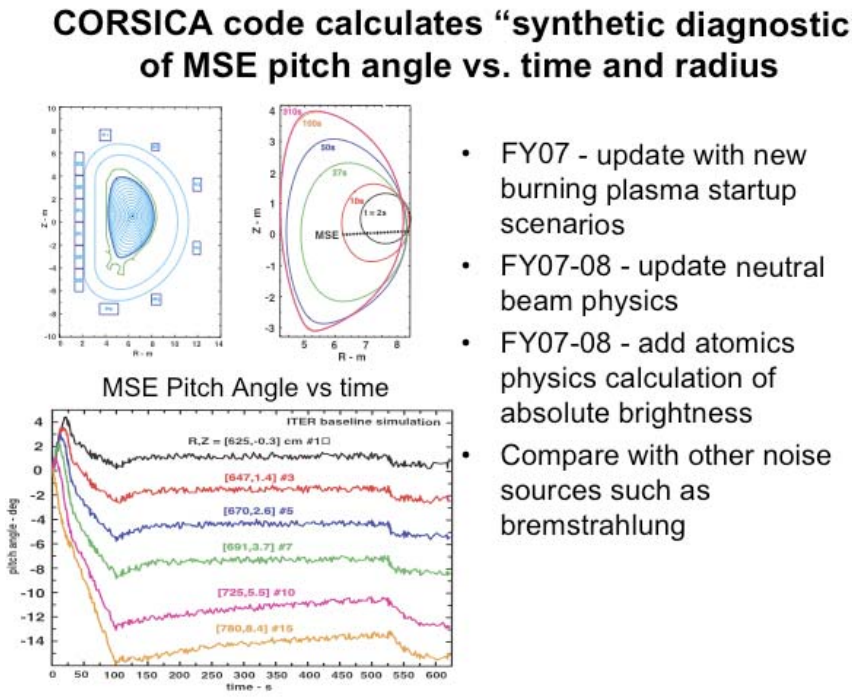

Figure C-1. Synthetic MSE diagnostic in the CORSICA code